AP 4018
FEB. 1989

# GAMMA SPECTROSCOPY

## WEEK 1:

FAMILIARIZE YOURSELF WITH THE EQUIPMENT AND THE COMPUTER-CONTROLLED MULTICHANNEL ANALYZER.

CHECK THE BACKGROUND AND DARK CURRENT RATES.

CHECK THE INFLUENCE OF THE PHOTOMULTIPLIER GAIN ON THE SPECTRUM.

RECORD THE SPECTRUM OF THE SIX SAMPLES: ($Co^{57}$, 122 KEV), ($Co^{60}$, 1173.2, 1332.5 KEV), ($Na^{22}$, 1.274 MEV), $Mn^{54}$, ($Cs^{137}$, .662 MEV)

EXAMINE THE ENERGY RESOLUTION OF YOUR SYSTEM.

EXAMINE AND EXPLAIN THE PEAKS OBSERVED FOR EACH SAMPLE

CALIBRATE YOUR MCA.

## WEEK 2:

RECORD THE SPECTRUM OF THE "MYSTERY SAMPLE" — TRY TO IDENTIFY IT FROM RADIATION TABLES

USING THE LABELED SOURCES, ABSOLUTELY CALIBRATE YOUR DETECTOR. BE SURE TO USE LEAD COLLIMATORS.

## WEEK 3:

READ THE HANDOUT ON THE ACTIVATION EXPERIMENTS AND USE YOUR MCA TO DETERMINE THE CONCENTRATIONS OF $MnSO_4 \cdot H_2O$ AND $NaCO_3$ IN YOUR SAMPLE.

# USE OF THE ORTEC SYSTEM

## DESCRIBTION:

The ORTEC system is a single channel analyzer counting system. It consists of a pre-amplifier, an amplifier, a single channel analyzer, and counter/timer. The following is a basic describtion and set-up guide for this equipment. You will need this equipment for more than just one lab therefore it is recommended that you keep this guide and bring it to every lab.

## MODEL 113 SCINTILLATION PREAMPLIFIER:

Basic operation as a pre-amplifier. The "INPUT CAP pF" switch will be in the "0" position unless otherwise stated.

## MODEL 485 AMPLIFIER:

Basic operation as a amplifier. The gain controls operate to amplify incoming signals. The coarse gain will double the size of any signal as the dial is increased. Fine gain also increases the gain but only within the constraintsof the coarse gain setting.

Place the other switches in "POS" and "UNIPOLAR" unless otherwise stated.

## MODEL 551 TIMING SINGLE-CHANNEL ANALYZER:

This unit can perform many functions from delaying the pulse train to discriminating the output. The SCA will be described by function consisting of appropriate controls.

### DELAY FUNCTION:

The incoming pulses from the amplifier can be delayed as much as 11 microsec. The range is determined by the toggle switch and the exact value by the "DELAY" dial. Under normal operation the toggle will be in the ".1-1.1usec" position and the "DELAY" dial locked in the "0" position. This will ensure minimum delay.

DISCRIMIATOR FUNCTION:

There are three (3) modes of discrimination:

TOGGLE SWITCH IN "INT"

Only the "LOWER LEVEL" dial is in opertion setting the lower level threshold in a range from 0 to 10V

TOGGLE SWITCH IN "NOR"

"LOWER LEVEL" dial and "UPPER LEVEL" dial act independently, therefore the upper threshold has to be greater than the lower threshold or there is not output. Both dials operate in a range from 0-10V.

TOGGLE SWITCH IN "WIN"

"LOWER LEVEL" dial acts as the threshold and the "WINDOW" dial is added to it. Lower level operates in a range of 0 - 10V and the window is 0 - 1 V. This allows the movement of the window by just changing the threshold.

MODEL 871 TIMER AND COUNTER:

Instrument consists of an 8-decade counter and an 8-decade presettable counter with time base. Operates as a counting device with the ability to count for specific units of time, rezero itself and count again.

DISPLAY SECTION:

OVFL: indicates if overflow has occurred in counter or timer

GATE: indicates unit is in counting condition

COUNTER: display is in counter condition

TIMER: display is in timer condition

SELECT: determines condition of display

TEST: illuminates all LED (00000008)

TIMER:

INC M & INC N: illuminates two LED in sequential number from 0 - 9, read as M times ten to the N . For example M = 5 and N = 2 would equal 500 or 5 times ten to the 2 used with one of the following.

TIME BASE SELECT: determines the unit of time to use with INC M & INC N. If selected to 0.1sec then the timed count would be 500 x 0.1 sec = 50 sec or if selected to MIN it would be 500 minutes. EXT is for an external timer.

DWELL: Determines the time between the end of the count and the beginning of the next. This will delay the count from 1 - 15 seconds. When in operation the count is always reset before new count. When in off the count does not resume.

STOP:

Pushbutton switch selects noncounting condition for both portions of the instrument.

RESET:

Pushbutton switch resets the internal registers for both

counting portions of the instrument and for the time base register and turns off the OVFL indicator.

COUNT:

Pushbutton switch enables counting condition for both portions of the instrument, provided the timer is not at its preset level.

If you have any other questions concerning the operation of the ORTEC equipment, consult the instructor or the technical manual.

BLOCK DIAGRAM

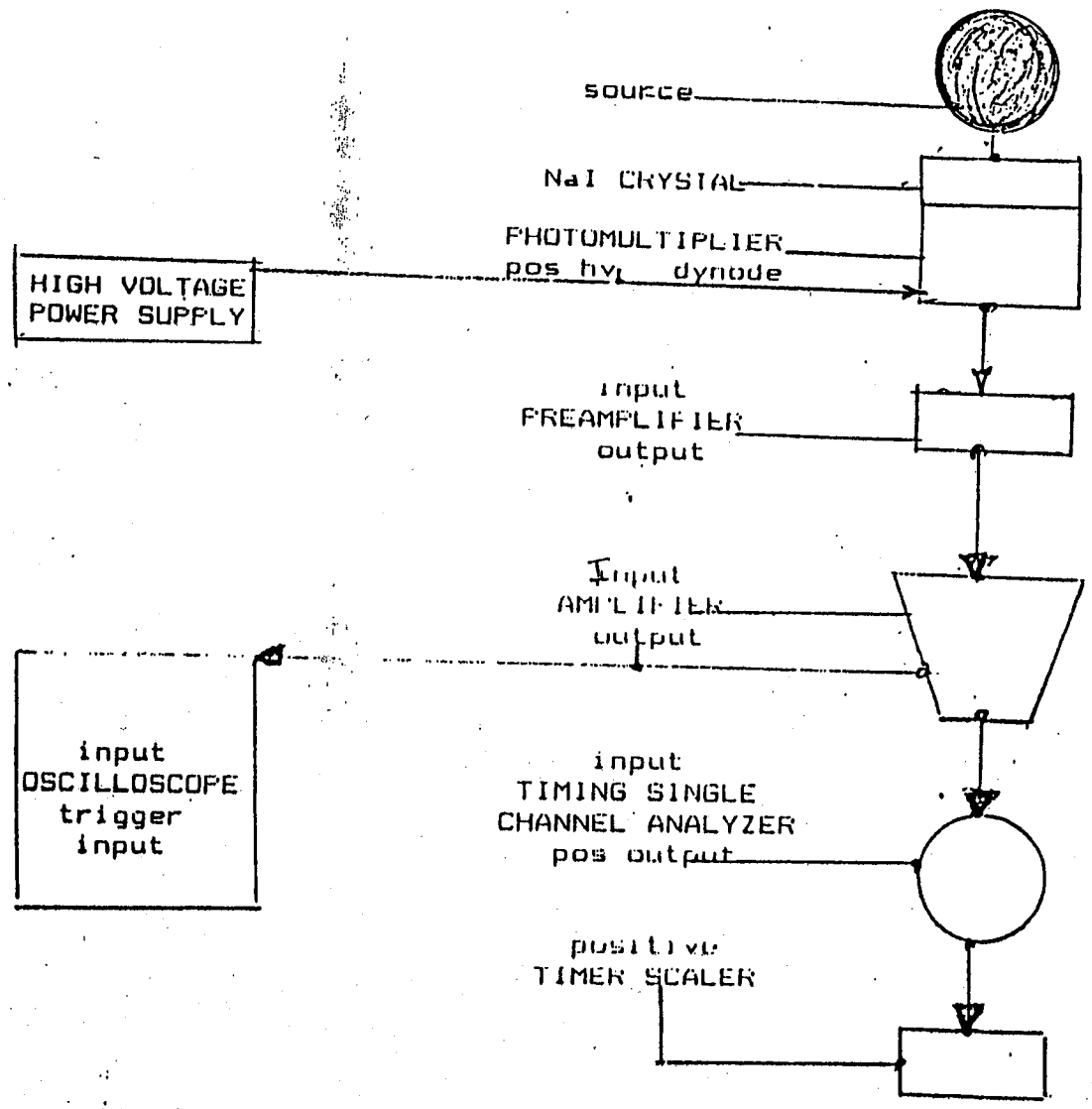

MEASUREMENT AND DETECTION OF RADIATION
N. TSOULFANIDIS (McGRAW-HILL, 1983)

# 6

# scintillation detectors

## 6.1 INTRODUCTION

Scintillators are materials—solids, liquids, gases—that produce sparks or scintillations of light when ionizing radiation passes through them. The first solid material to be used as a particle detector was a scintillator. It was used by Rutherford, in 1910, in his alpha-scattering experiments. In his experimental setup, alpha particles hit a zinc sulfide screen and produced scintillations, which were counted with or without the help of a microscope—a very inefficient process, inaccurate and time consuming. The method was abandoned for about 30 years and was remembered again when advanced electronics made possible amplification of the light produced in the scintillator.

The amount of light produced in the scintillator is very small. It must be amplified before it can be recorded as a pulse or in any other way. The amplification or multiplication of the scintillator's light is achieved with a device known as the *photomultiplier tube* (or *phototube*). Its name denotes its function: It accepts a small amount of light, amplifies it many times, and delivers a strong pulse at its output. Amplifications of the order of $10^6$ are common for many commercial photomultiplier tubes. Apart from the phototube, a detection system that uses a scintillator is no different from any other (Fig. 6.1).

The operation of a scintillation counter may be divided into two broad steps:

1. Absorption of incident radiation energy by the scintillator and production of photons in the visible part of the electromagnetic spectrum
2. Amplification of the light by the photomultiplier tube and production of the output pulse

The sections that follow analyze these two steps in detail. The different types of scintillators are divided, for the present discussion, into three groups:

1. Inorganic scintillators
2. Organic scintillators
3. Gaseous scintillators

## 6.2 INORGANIC SCINTILLATORS (CRYSTAL SCINTILLATORS)

Most of the inorganic scintillators are crystals of the alkali metals, in particular alkali iodides, that contain a small concentration of an impurity. Examples are NaI(Tl), CsI(Tl), CsI(Na), LiI(Eu), and $CaF_2$(Eu). The element in parentheses is the impurity or activator. Although the activator has a relatively small concentration—e.g., thallium in NaI(Tl) is $10^{-3}$ on a per mole basis—it is the agent that is responsible for the luminescence of the crystal.

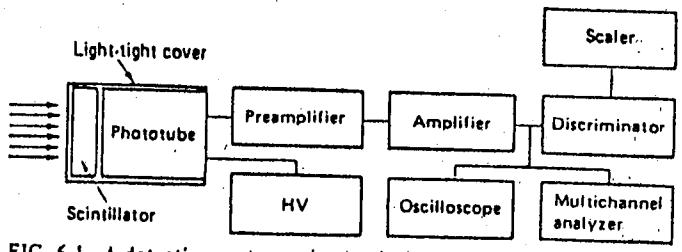


FIG. 6.1 A detection system using a scintillator.

### 6.2.1 The Mechanism of the Scintillation Process

The luminescence of inorganic scintillators can be understood in terms of the allowed and forbidden energy bands of a crystal. The electronic energy states of an atom are discrete energy levels, which in an energy level diagram are represented as discrete lines. In a crystal, the allowed energy states widen into bands (Fig. 6.2). In the ground state of the crystal, the uppermost allowed band that contains electrons is completely filled. This is called the *valence band.* The next allowed band is empty (in the ground state) and is called the *conduction band.* An electron may obtain enough energy from incident radiation to move from the valence to the conduction band. Once there, the electron is free to move anywhere in the lattice. The removed electron leaves behind a hole in the valence band, which can also move. Sometimes, the energy given to the electron is not sufficient to raise it to the conduction band. Instead, the electron remains electrostatically bound to the hole in the valence band. The electron-hole pair thus formed is called an *exciton.* In terms of energy states, the exciton corre-

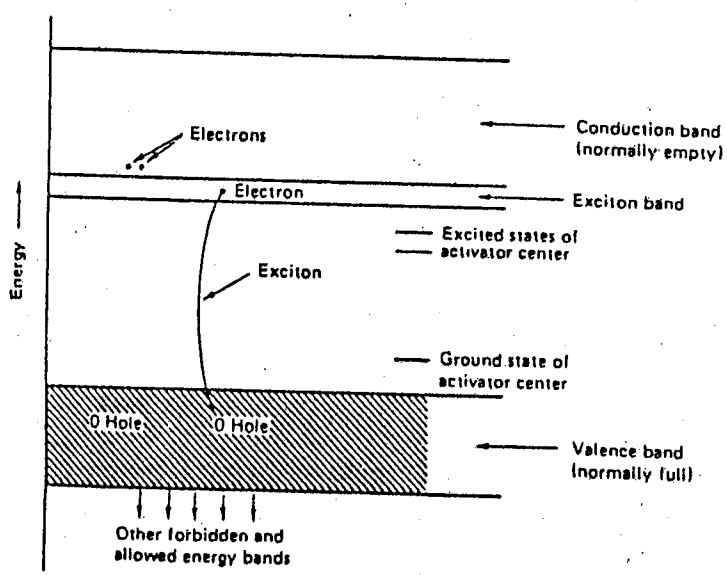


FIG. 6.2 Allowed and forbidden energy bands of a crystal.



corresponds to elevation of the electron to a state higher than the valence but lower than the conduction band. Thus, the exciton states form a thin band, with upper level coinciding with the lower level of the conduction band (Fig. 6.2). The width of the exciton band is of the order of 1 eV, while the gap between valence and conduction bands is of the order of 8 eV.

In addition to the exciton band, energy states may be created between valence and conduction bands because of crystal imperfections or impurities. Particularly important are the states created by the activator atoms such as thallium. The activator atom may exist in the ground state or in one of its excited states. Elevation to an excited state may be the result of a photon absorption or of the capture of an exciton or of the successive capture of an electron and a hole. The transition of the impurity atom from the excited to the ground state, if allowed, results in the emission of a photon in times of the order of $10^{-8}$ s. If this photon has a wavelength in the visible part of the electromagnetic spectrum, it contributes to a scintillation. Thus, production of a scintillation is the result of the occurrence of these events:

1 Ionizing radiation passes through the crystal.
2 Electrons are raised to the conduction band.
3 Holes are created in the valence band.
4 Excitons are formed.
5 Activation centers are raised to the excited states by absorbing electrons, holes, and excitons.
6 Deexcitation is followed by the emission of a photon.

The light emitted by a scintillator is primarily the result of transitions of the activator atoms, and not of the crystal. Since most of the incident energy goes to the lattice of the crystal—eventually becoming heat—the appearance of luminescence produced by the activator atoms means that energy is transferred from the host crystal to the impurity. For NaI(Tl) scintillators, about 12 percent of the incident energy appears as thallium luminescence.[1]

The magnitude of the light output and the wavelength of the emitted light are two of the most important properties of any scintillator. The light output affects the number of photoelectrons generated at the input of the photomultiplier tube (see Sec. 6.5), which in turn affects the pulse height produced at the output of the counting system. Information about the wavelength is necessary in order to match the scintillator with the proper photomultiplier tube. Emission spectra of NaI(Tl), CsI(Na), and CsI(Tl) are shown in Fig. 6.3. Also shown in Fig. 6.3 are the responses of two phototube cathode materials. Table 6.1 gives the most important properties of some inorganic scintillators.

The light output of the scintillators depends on temperature. Figure 6.4 shows the temperature response of NaI(Tl), Cs(Tl), and CsI(Na).

### 6.2.2 Time Dependence of Photon Emission

Since the photons are emitted as a result of decays of excited states, the time of their emission depends on the decay constants of the different states involved. Experiments show that the emission of light follows an exponential decay law of the form

$$N(t) = N_0 e^{-t/T} \tag{6.1}$$

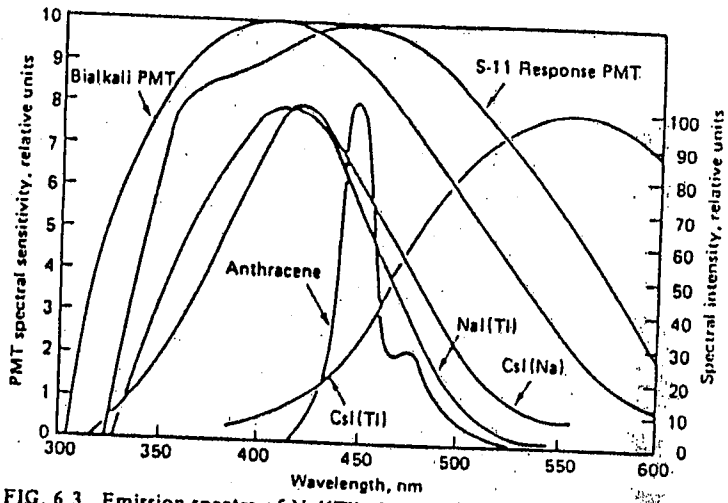


FIG. 6.3 Emission spectra of NaI(Tl), CsI(Tl), CsI(Na), and anthracene, compared to the spectral response of two photocathode materials. (From HARSHAW Research Laboratory Report.)

where $N(t)$ = number of photons emitted at time $t$

$T$ = decay time of the scintillator (see Table 6.1)

Most of the excited states in a scintillator have essentially the same lifetime $T$. There are, however, some states with longer lifetimes contributing a slow component in the decay of the scintillator known as *afterglow*. It is present to some extent in all inorganic scintillators and may be important in certain measurements where the integrated output of the phototube is used. Two scintillators with negligible afterglow are $CaF_2$(Eu) and $Bi_4Ge_3O_{12}$ (bismuth orthogermanate).

In a counting system using a scintillator, the light produced by the crystal is amplified by a photomultiplier tube and is transformed into an electric current having the exponential behavior given by Eq. 6.1. This current is fed into an RC circuit (see Sec. 10.2) as shown in Fig. 6.5, and a voltage pulse is produced of the form

$$V(t) = V_\infty(e^{-t/RC} - e^{-t/T}) \tag{6.2}$$

TABLE 6.1 Properties of Certain Inorganic Scintillators

| Material | Wavelength of maximum emission (nm) | Scintillation efficiency (relative, %) | Decay time (μs) | Density ($10^3$ kg/m) |
|---|---|---|---|---|
| NaI(Tl) | 410 | 100 | 0.23 | 3.67 |
| $CaF_2$(Eu) | 435 | 50 | 0.94 | 3.18 |
| CsI(Na) | 420 | 80 | 0.63 | 4.51 |
| CsI(Tl) | 565 | 45 | 1.80 | 4.51 |
| $Bi_4Ge_3O_{12}$ | 480 | 8 | 0.30 | 7.13 |
| $CdWO_4$ | 530 | 20 | 0.90 | 7.90 |
| LiI(Eu) | 470 | 30 | 0.94 | 3.49 |



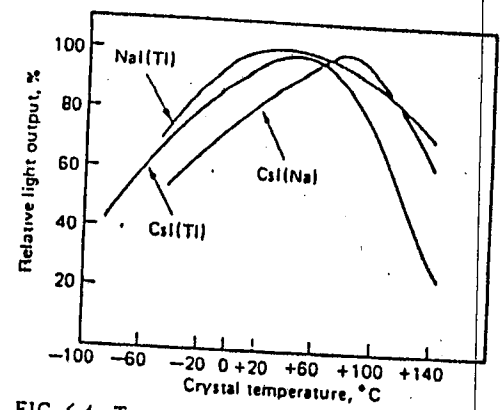


FIG. 6.4 Temperature dependence of light output of NaI(Tl), CsI(Tl), and CsI(Na). (From HARSHAW Research Laboratory Report.)

In practice, the value of $RC$ is selected to be of the order of a few hundreds of microseconds. Thus, for short times—i.e., $T \ll RC$, which is the timespan of interest—Eq. 6.2 takes the form

$$V(t) = V_\infty(1 - e^{-t/T}) \tag{6.2a}$$

Notice that the rate at which the pulse rises (risetime) is determined by the decay time $T$. In certain measurements, e.g., coincidence-anticoincidence measurements (Chap. 10), the timing characteristics of the pulse are extremely important.

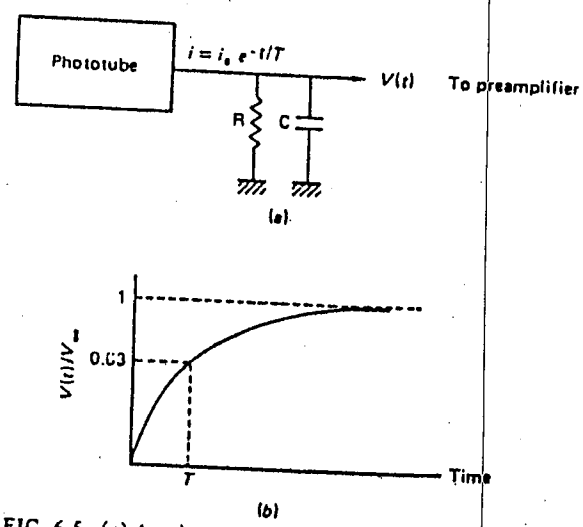


FIG. 6.5 (*a*) A voltage pulse results from the exponential current. (*b*) The shape of the pulse for $RC \gg T$.

### 6.2.3 Important Properties of Certain Inorganic Scintillators

NaI(Tl)

NaI(Tl) is the most commonly used scintillator for gamma rays. It has been produced in single crystals of up to 0.75 m (~30 in) in diameter and considerable thickness (0.25 m ≈ 10 in). Its relatively high density ($3.67 \times 10^3$ kg/m$^3$) and high atomic number combined with the large volume make it a $\gamma$-ray detector with very high efficiency. Although semiconductor detectors (Chaps. 7 and 12) have better energy resolution, they cannot replace the NaI(Tl) in experiments where large detector volumes are needed.

The emission spectrum of NaI(Tl) peaks at 410 nm, and the light-conversion efficiency is the highest of all the inorganic scintillators (Table 6.1). As a material, NaI(Tl) has many undesirable properties. It is brittle and sensitive to temperature gradients and thermal shocks. It is also so hygroscopic that it should be kept encapsulated at all times. NaI always contains a small amount of potassium, which creates a certain background because of the radioactive $^{40}$K.

CsI(Tl)

CsI(Tl) has a higher density ($4.51 \times 10^3$ kg/m$^3$) and higher atomic number than NaI; therefore its efficiency for gamma detection is higher. The light-conversion efficiency of CsI(tl) is about 45 percent of that for NaI(Tl) at room temperature. At liquid nitrogen temperatures (77 K), pure CsI has a light output equal to that of NaI(Tl) at room temperature and a decay constant equal to $10^{-8}$ s.[2] The emission spectrum of CsI(Tl) extends from 420 to about 600 nm.

CsI is not hygroscopic. Being softer and more plastic than NaI, it can withstand severe shocks, acceleration, and vibration, as well as large temperature gradients and sudden temperature changes. These properties make it suitable for space experiments. Finally, CsI does not contain potassium.

CsI(Na)

The density and atomic number of CsI(Na) are the same as those of CsI(Tl). The light-conversion efficiency is about 85 percent of that for NaI(Tl). Its emission spectrum extends from 320 to 540 nm (see Fig. 6.3). CsI(Na) is slightly hygroscopic.

$CaF_2$(Eu)

$CaF_2$(Eu) consists of low-atomic-number materials, and for this reason makes an efficient detector for $\beta$ particles[3] and x-rays[4] with low gamma sensitivity. It is similar to Pyrex and can be shaped to any geometry by grinding and polishing. Its insolubility and inertness make it suitable for measurements involving liquid radioisotopes. The light-conversion efficiency of $CaF_2$(Eu) is about 50 percent of that for NaI(Tl). The emission spectrum extends from about 405 to 490 nm.

LiI(Eu)

LiI(Eu) is an efficient thermal-neutron detector through the reaction $^6_3$Li$(n, \alpha)^3_1$H. The alpha particle and the triton, both charged particles, produce the scintillations. LiI has a density of $4.06 \times 10^3$ kg/m$^3$, decay time of about 1.1 $\mu$s, and emission spectrum peaking at 470 nm. Its conversion efficiency is about one-third of that for NaI. It is very hygroscopic and is subject to radiation damage as a result of exposure to neutrons.



OTHER INORGANIC SCINTILLATORS

Many other scintillators have been developed for special applications. Examples are $Bi_4Ge_3O_{12}$, $CdWO_4$, and more recently[5] $MF_2:UF_4:CeF_3$, where M stands for one of the following: Ca, Sr, Ba. This last scintillator containing 2 percent $UF_4$ and using Ce as the fluorescing agent has been used for detection of fission fragments.

## 6.3 ORGANIC SCINTILLATORS

The materials that are efficient *organic scintillators* belong to the class of aromatic compounds. They consist of planar molecules made up of benzenoid rings. Two examples are toluene and anthracene, having the structures shown in Fig. 6.6.

Organic scintillators are formed by combining appropriate compounds. They are classified as unitary, binary, ternary, and so on, depending on the number of compounds in the mixture. The substance with the highest concentration is called the *solvent*. The others are called *solutes*. A binary scintillator consists of a solvent and a solute, while a ternary scintillator is made of a solvent, a primary solute, and a secondary solute. Table 6.2 lists the most common compounds used.

### 6.3.1 The Mechanism of the Scintillation Process

The production of light in organic scintillators is the result of molecular transitions. Consider the energy-level diagram of Fig. 6.7, which shows how the potential energy of a molecule changes with interatomic distance. The ground state of the molecule is at point $A$, which coincides with the minimum of the potential energy. Ionizing radiation passing through the scintillator may give energy to the molecule and raise it to an excited state, i.e., the transition $A_0 \rightarrow A_1$ may occur. The position $A_1$ is not the point of minimum energy. The molecule will release energy through lattice vibrations (that energy is eventually dissipated as heat) and move to point $B_1$. The point $B_1$ is still an excited state and, in some cases, the molecule will undergo the transition $B_1 \rightarrow B_0$ accompanied by the emission of a photon with energy equal to $E_{B_1} - E_{B_0}$. This transition, if allowed, takes place at times of the order $10^{-8}$ s. It should be noted that the energy of the emitted photon ($E_{B_1} - E_{B_0}$) is less than the energy that caused the excitation ($E_{A_1} - E_{A_0}$). This difference is very important because otherwise the emission spectrum of the scintillator would completely coincide with its absorption spectrum and no scintillations would be produced. A more detailed description of the scintillation process is given in the references (see Birks and reference 6).

One of the important differences between inorganic and organic scintillators is in the response time, which is less than 10 ns for the latter (response time of inorganic scintillators is ~1 $\mu$s, see Table 6.1) and makes them suitable for fast timing measurements (see Chap. 10). Table 6.3 lists important properties of some organic scintillators.

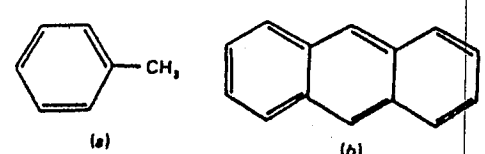


FIG. 6.6 Molecular structure of (*a*) toluene and (*b*) anthracene.

## 6.6 THE PHOTOMULTIPLIER TUBE

### 6.6.1 General Description

The photomultiplier tube or phototube is an integral part of a scintillation counter. Without the amplification produced by the photomultiplier, a scintillator is uesless as a radiation detector. The photomultiplier is essentially a fast amplifier, which in times of $10^{-9}$ s amplifies an incident pulse of visible light by a factor of $10^6$ or more.

A photomultiplier consists of an evacuated glass tube with a photocathode at its entrance and several dynodes in the interior (Fig. 6.13). The photons produced in the scintillator enter the phototube and hit the photocathode, which is made of a material that emits electrons when light strikes it. The electrons emitted by the photocathode are guided, with the help of an electric field, towards the first dynode, which is coated with a substance that emits secondary electrons, if electrons impinge upon it. The secondary electrons from the first dynode move towards the second, from there towards the third, and so on. Typical commercial phototubes may have up to 15 dynodes. The production of secondary electrons by the successive dynodes results in a final amplification of the number of electrons as shown in the next section.

The electrons produced in the phototube are directed from one dynode to the next by an electric field established by applying a successively increasing positive high voltage to each dynode. The voltage difference between two successive dynodes is of the order of 80–120 V (see Sec. 6.6.2).

The photocathode material used in most commercial phototubes is a compound of cesium and antimony (Cs-Sb). The material used to coat the dynodes is either Cs-Sb or silver-magnesium (Ag-Mg). The secondary emission rate of the dynodes depends not only on the type of surface but also on the voltage applied.

A very important parameter of every photomultiplier tube is the spectral sensitivity of its photocathode. For best results, the spectrum of the scintillator should match the sensitivity of the photocathode. The Cs-Sb surface has a maximum sensitivity at 440 nm, which agrees well with the spectral response of most scintillators (Tables 6.1 and 6.3). Such a response, called S-11, is shown in Fig. 6.3. Other responses of commercial phototubes are known as S-13, S-20, etc.

Another important parameter of a phototube is the magnitude of its *dark current*. The dark current consists mainly of electrons emitted by the cathode after

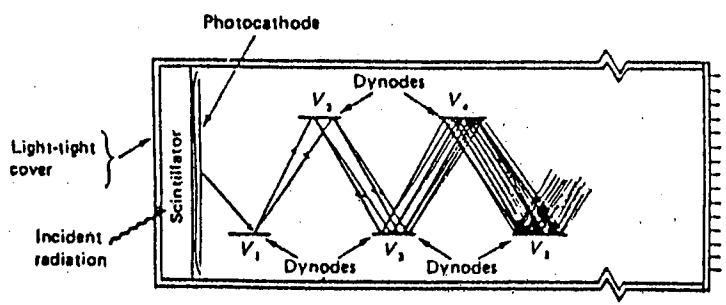


FIG. 6.13 Schematic diagram of the interior of a photomultiplier tube.



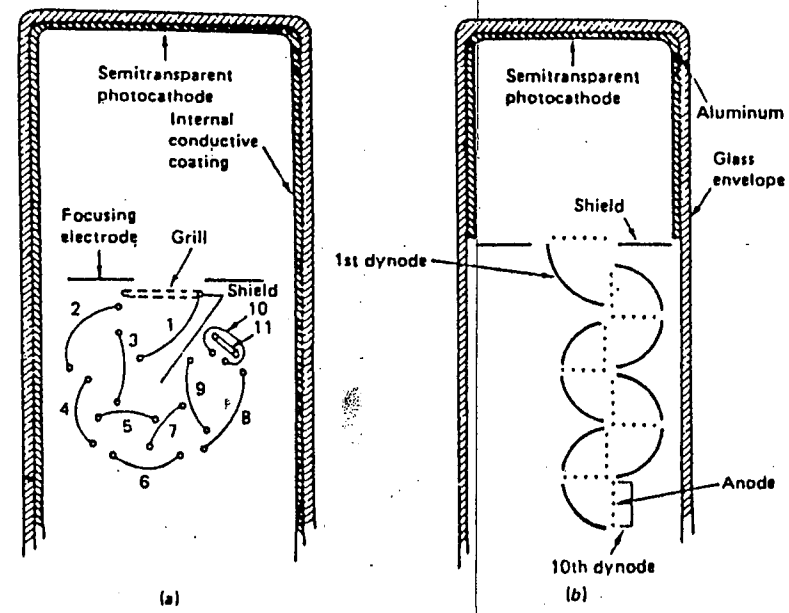


FIG. 6.14 Two dynode arrangements in commercial phototubes: (*a*) Model 6342 RCA, 1–10 are dynodes, 11 is anode; (*b*) Model 6292 DuMont.

thermal energy is absorbed. This process is called *thermionic emission*, and a 50-mm-diameter photocathode may release in the dark as many as $10^5$ electrons/s at room temperature. Cooling of the cathode reduces this source of noise by a factor of about 2 per 10–15°C reduction in temperature. Thermionic emission may also take place from the dynodes and the glass wall of the tube, but this contribution is small. Electrons may be released from the photocathode as a result of its bombardment by positive ions coming from ionization of the residual gas in the tube. Finally, light emitted as a result of ion recombination may release electrons upon hitting the cathode or the dynodes. Obviously, the magnitude of the dark current is important in cases where the radiation source is very weak. Both the dark current and the spectral response should be considered when a phototube is to be purchased.

Recall that the electrons are guided from one dynode to the next by an electric field. If a magnetic field is present, it may deflect the electrons in such a way that not all of them hit the next dynode, and the amplification is reduced. Even the earth's weak magnetic field may sometimes cause this undesirable effect. The influence of the magnetic field may be minimized by surrounding the photomultiplier tube with a cylindrical sheet of metal, called *μ-metal*. The μ-metal is commercially available in various shapes and sizes.

Commercial photomultiplier tubes are made with a variety of geometrical arrangements of photocathode and dynodes. In general, the photocathode is deposited as a semitransparent layer on the inner surface of the end window of the phototube (Fig. 6.14). The external surface of the window is, in most phototubes, flat for easier

optical coupling with the scintillator (see Sec. 6.7). Two different geometries for the dynodes are shown in Fig. 6.14.

### 6.6.2 Electron Multiplication in a Photomultiplier

The electron multiplication $M$ in a photomultiplier can be written as:

$$M = (\theta_1\epsilon_1)(\theta_2\epsilon_2)\cdots(\theta_n\epsilon_n) \tag{6.3}$$

where

$n$ = number of dynodes

$$\epsilon_i = \frac{\text{number of electrons collected by } i\text{th dynode}}{\text{number of electrons emitted by } (i-1)\text{th dynode}}$$

$$\theta_i = \frac{\text{number of electrons emitted by } i\text{th dynode}}{\text{number of electrons impinging upon } i\text{th dynode}}$$

If $\theta_i$ and $\epsilon_i$ are constant for all dynodes, then

$$M = (\theta\epsilon)^n \tag{6.4}$$

The quantity $\epsilon$ depends on the geometry. The quantity $\theta$ depends on the voltage between two successive dynodes and on the material of which the dynode is made. The dependence of $\theta$ on voltage is of the form

$$\theta = kV^a \tag{6.5}$$

where $V = V_i - V_{i-1}$ = potential difference between two successive dynodes, assumed the same for dynodes

$k, a$ = constants (the value of $a$ is about 0.7)

Using Eq. 6.5, the multiplication $M$ becomes

$$M = \epsilon^n(kV^a)^n = CV^{an} \tag{6.6}$$

where $C = (\epsilon k)^n$ = constant, independent of the voltage.

Equation 6.6 indicates that the value of $M$ increases with the voltage $V$ and the number of stages $n$. The number of dynodes is limited, because as $n$ increases, the charge density between two dynodes distorts the electric field and hinders the emission of electrons from the previous dynode with the lower voltage. In commercial photomultipliers, the number of dynodes is 10 or more. If one takes $n = 10$ and $\epsilon\theta = 4$, a typical value, the value of $M$ becomes equal to $10^6$.

To apply the electric field to the dynodes, a power supply provides a voltage adequate for all the dynodes. A voltage divider, usually an integral part of the preamplifier, distributes the voltage to the individual dynodes. When reference is made to *phototube voltage*, one means the total voltage applied. For example, if 900 V are applied to a phototube with 10 dynodes, the voltage between any two dynodes is 100 V.



## 6.7 ASSEMBLY OF A SCINTILLATION COUNTER AND THE ROLE OF LIGHT PIPES

A scintillation counter consists of the scintillator and the photomultiplier tube. It is extremely important that these two components be coupled in such a way that a maximum amount of light enters the phototube and strikes the photocathode. This section presents a brief discussion of the problems encountered during the assembly of a scintillation counter, with some of the methods used to solve them.

A solid scintillator is coupled to the photomultiplier through the end window of the tube (Fig. 6.15). During the transfer from the scintillator to the photocathode, light may be lost by leaving through the sides and front face of the scintillator, or by being reflected back to the scintillator when it hits the window of the phototube.

To avoid loss of light through the sides and front face, the scintillator is painted with a material that reflects toward the crystal the light that would otherwise escape. Examples of reflecting materials commercially available are alpha alumina and $Al_2O_3$.

To avoid reflection of light from the end window of the phototube, a transparent viscous fluid (such as Dow-Corning 200 Silicone fluid) is placed between the scintillator and the phototube (Fig. 6.15). The optical fluid minimizes reflection because it reduces the change of the index of refraction during the passage of light from the scintillator to the phototube. A sharp change in the index of refraction results in a small critical angle of reflection, which in turn increases total reflection.

In certain experiments, the scintillator has to be a certain distance away from the photocathode. Such is the case if the phototube should be protected from the radiation impinging upon the scintillator or from a magnetic field. Then a *light pipe* is interposed between the scintillator and the phototube. The light pipe is made of a material transparent to the light of the scintillator. Lucite, quartz, plexiglass, and glass have been used in many applications to form light pipes of different lengths and shapes. Light pipes of several feet—sometimes with bends—have been used with success. The optical coupling of the light pipe at both ends is accomplished by the same methods used to couple the scintillator directly to the phototube.

One of the major reasons for using scintillators is their availability in large sizes. In fact, commercially available scintillators are larger than the biggest commercial photomultipliers. In cases where the scintillator is too large, multiple phototubes are coupled to the same crystal. Figure 6.16 shows a NaI(Tl) crystal coupled to six photomultipliers.

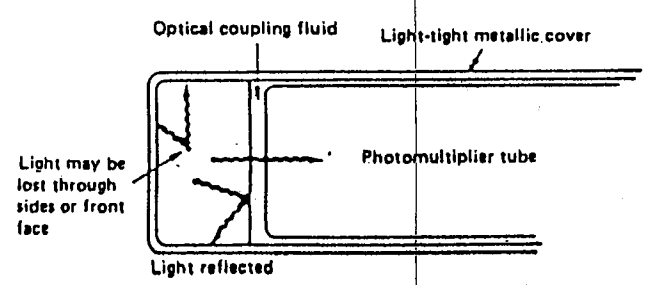


FIG. 6.15 Assembly of a scintillation counter.

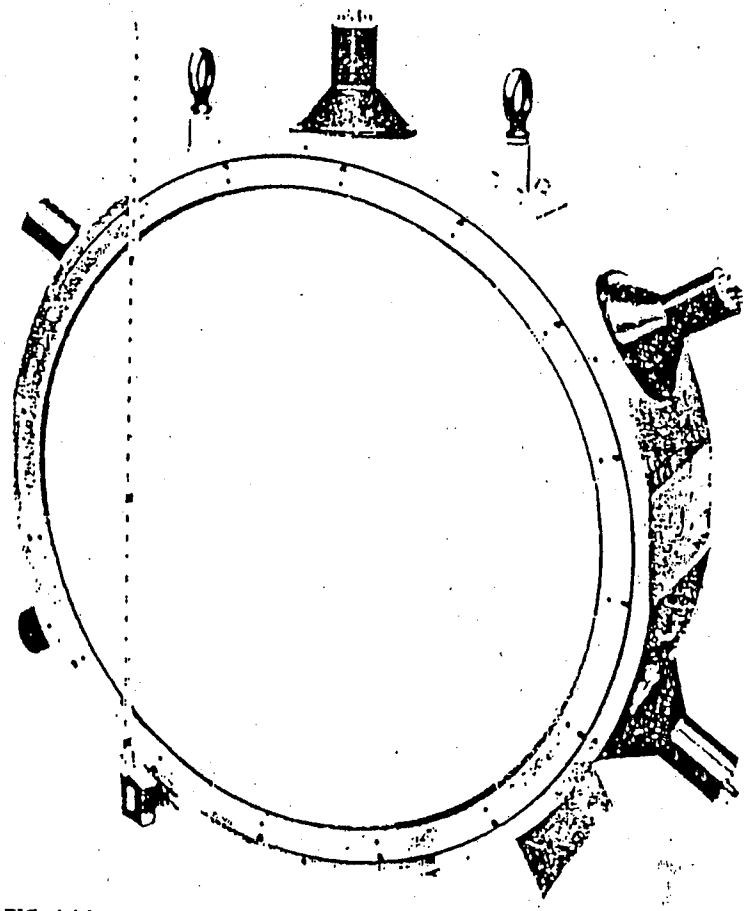

FIG. 6.16 A special 30-in (0.762-m) diameter scintillator crystal coupled to six photomultiplier tubes (from HARSHAW Chemical Company).

When a liquid scintillator is used, the phototube is optically coupled to the scintillator through a window of the vessel containing the liquid scintillator. The efficiency of such a counting system increases by using a large volume of liquid and more than one photomultiplier tube (Fig. 6.17).

## 6.8 DEAD TIME OF SCINTILLATION COUNTERS

The *dead time* or *resolving time* is the minimum time that can elapse after the arrival of two successive particles and still result in two separate pulses (see Sec. 2.20). For a scintillation counter this time is equal to the sum of three time intervals:

1 Time it takes to produce the scintillation, essentially equal to the decay time of the scintillator (see Eq. 6.1 and Tables 6.1 and 6.3).



2 Time it takes for electron multiplication in the phototube, of the order of 20–40 ns.
3 Time it takes to amplify the signal and record it by a scaler. The recovery time of commercial scalers is of the order of 1 $\mu$s. The time taken for amplification and discrimination is negligible.

By adding the three above components, the resulting dead time of a scintillation counter is of the order of 1–5 $\mu$s. This is much shorter than the dead time of gas-filled counters, which is of the order of tens to hundreds of microseconds.

Scintillators are detectors with fast response. As seen in Tables 6.1 and 6.3, the risetime of the pulse is very short for all of them. Short risetime is important in measurements that depend on the time of arrival of the particle (see Chap. 10).

## 6.9 SOURCES OF BACKGROUND IN A SCINTILLATION COUNTER

One of the major sources of background in a scintillation counter is the dark current of the phototube (see Sec. 6.6.1). Other background sources are naturally occurring radioisotopes, cosmic rays, and phosphorescing substances.

The holder of a liquid scintillator may contain small amounts of naturally occurring isotopes. In particular, $^{40}$K is always present (isotopic abundance of $^{40}$K is 0.01 percent). Another isotope, $^{14}$C, is a constituent of contemporary organic materials. Solvents, however, may be obtained from petroleum, consisting of hydrocarbons without $^{14}$C.

The term *phosphorescence* refers to delayed emission of light as a result of deexcitation of atoms or molecules. Phosphorescent half-lives may extend to hours. This source of background may originate in phosphorescent substances contained in the glass of the phototube, the walls of the sample holder, or the sample itself.

*Cosmic rays*, which are highly energetic charged particles, produce background in all types of detectors, and scintillators are no exception. The effect of cosmic-ray background, as well as that of the other sources mentioned earlier, will be reduced if two counters are used in coincidence or anticoincidence.

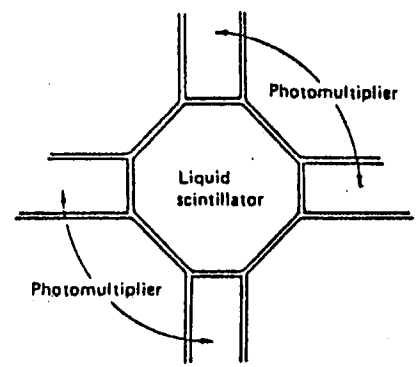


FIG. 6.17 A counting system using a liquid scintillator and four photomultiplier tubes.

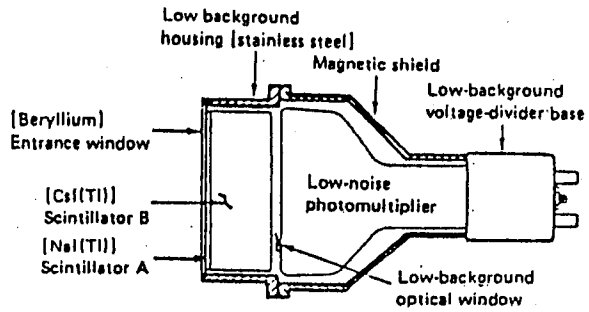


FIG. 6.18 A Phoswich detector (from HARSHAW Chemical Co.).

## 6.10 THE PHOSWICH DETECTOR

The phoswich detector is used for the detection of low-level radiation in the presence of considerable background. It consists of two different scintillators coupled together and mounted on a single photomultiplier tube.[1] By utilizing the difference in the decay constants of the two phosphors, differentiation between events taking place in the two detectors is possible. The combination of crystals used depends on the types of particles being present in the radiation field under investigation.

The basic structure of a phoswich detector is shown in Fig. 6.18. A thin scintillator (scintillator A) is coupled to a larger crystal (scintillator B), which in turn is coupled to the cathode of a single phototube. Two examples of scintillators used are these:

1 NaI(Tl) is the thin scintillator (A) and CsI(Tl) is the thick one (B). Pulses originating in the two crystals are differentiated based on the difference between the 0.25-$\mu$s decay constant of the NaI(Tl) and the 1-$\mu$s decay constant of the CsI(Tl). Slow pulses come from particles losing energy in the CsI(Tl) or in both crystals simultaneously. In a mixed low-energy–high-energy photon field, the relatively fast pulses of the NaI(Tl) will come from the soft component of the radiation. [Soft photons will not reach the CsI(Tl).] Phoswich detectors of this type have been used in x-ray and $\gamma$-ray astronomy, in detection of plutonium in the environment, and in other cases of mixed-radiation fields.

2 $CaF_2$(Eu) is the thin scintillator (A) and NaI(Tl) is the thick one (B). This combination is used for measurements of low-energy beta particles in the presence of a gamma background. The thin (0.1 mm) $CaF_2$(Eu) crystal detects the betas, but is essentially transparent to gammas because of its relatively low atomic number and thickness. A quartz window is usually placed between the two scintillators to stop the betas that did not deposit all their energy in the $CaF_2$(Eu). The fast pulses of the NaI(Tl), which are due to gammas, are time-discriminated against the slower pulses from the $CaF_2$(Eu) ($\tau = 0.94$ $\mu$s). Thus, the background due to gammas is reduced.

## PROBLEMS

6.1 If the dead time of a detection using a scintillator is 1 $\mu$s, what is the gross counting rate that will result in a loss of 2 percent of the counts?



6.2 A typical dead time for a scintillation detector is 5 $\mu$s. For a gas counter, the corresponding number is 200 $\mu$s. If a sample counted with a gas counter results in 8 percent loss of gross counts due to dead time, what is the corresponding loss in a scintillation counter that records the same gross counting rate?

6.3 A parallel beam of 1.5-MeV gammas strikes a 25-mm thick NaI crystal. What fraction of these gammas will have at least one interaction in the crystal ($\mu = 0.0047$ m$^2$/kg)?

6.4 What is the range of 2-MeV electrons in a plastic scintillator? Assume that the composition of the scintillator is $C_{10}H_{11}$ ($\rho = 1.02 \times 10^3$ kg/m$^3$).

6.5 Consider two electrons, one with kinetic energy 1 MeV, the other with 10 MeV. Which electron will lose more energy going through a 1-mm-thick plastic scintillator? Consider both ionization and radiation loss. Composition of the scintillator is given in Prob. 6.4. For radiation loss, use

$$Z_{\text{eff}} = \frac{N_H Z_H^2 + N_C Z_C^2}{N_H Z_H + N_C Z_C}$$

6.6 A phoswich detector consists of a 1-mm thick NaI(Tl) scintillator coupled to a 25-mm-thick CsI(Tl) scintillator. A 0.1-mm-thick beryllium window protects the NaI(Tl) crystal. If the detector is exposed to a thin parallel beam of 150-keV x-rays and 1.5-MeV $\alpha$ rays, what are the fractions of interactions of each type of photon in each scintillator?

## BIBLIOGRAPHY

Birks, J. B., *The Theory and Practice of Scintillation Counting*, McMillan Co., New York, 1964.
Fenyves, E., and Haiman, O., *The Physical Principles of Nuclear Radiation Measurements*, Academic Press, New York, 1969.
Price, W. J., *Nuclear Radiation Detection*, McGraw-Hill, New York, 1964.
Snell, A. H. (ed.), *Nuclear Instruments and Their Uses*, Wiley, New York, 1962.

## REFERENCES

1 Heath, R. L., Hofstadter, R., and Hughes, E. B., *Nucl. Instr. Meth.* 162:431 (1979). (Review article listing 127 references.)
2 Aliaga-Kelly, D., and Nicoll, D. R., *Nucl. Instr. Meth.* 43:110 (1966).
3 Colmenares, C., Shapiro, E. G., Barry, P. E., and Prevo, C. T., *Nucl. Instr. Meth.* 114:277 (1974).
4 Campbell, M., Ledingham, K. W. D., Baillie, A. D., and Lynch, J. G., *Nucl. Instr. Meth.* 137: 235 (1976).
5 Catalano, E., and Czirr, J. B., *Nucl. Instr. Meth.* 143:61 (1977).
6 Brooks, F. D., *Nucl. Instr. Meth.* 162:477 (1979). (Review article listing 274 references.)
7 Bollinger, L. M., and Thomas, G. E., *Rev. Sci. Instr.* 28:489 (1957).
8 Hellstrom, J., and Beshai, S., *Nucl. Instr. Meth.* 101:267 (1972).
9 Bergere, R., Bell, H., and Veyssiere, A., *Nucl. Phys.* A121:463 (1968).
10 Swank, R. K., *Ann. Rev. Nucl. Sci.* 4:111 (1954).
11 Walker, J. K., *Nucl. Instr. Meth.* 68:131 (1969).
12 Moszynski, M., and Bengtson, B., *Nucl. Instr. Meth.* 142:417 (1977).
13 Moszynski, M., and Bengtson, B., *Nucl. Instr. Meth.* 158:1 (1979).
14 Eriksson, L. A., Tsai, C. M., Cho, Z. H., and Hurlbut, C. R., *Nucl. Instr. Meth.* 122:373 (1974).
15 Becker, J., Eriksson, L., Monberg, L. C., and Cho, Z. H., *Nucl. Instr. Meth.* 123:199 (1975).
16 Muga, M. L., Burnsed, D. J., Steeger, W. E., and Taylor, H. E., *Nucl. Instr. Meth.* 83:135 (1970).

and the detector aperture has a radius of 20 mm ($F = 1$). What is the standard error of the result if the error of the gross counting rate is known with an accuracy of ±5 percent and the background with ±3 percent? Dead time is 1 μs.

8.12 A point isotropic source is located at the center of a hemispherical $2\pi$ counter. The efficiency of this detector for the particles emitted by the source is 85 percent. The saturation backscattering factor is 1.5. The background 25 ± 1 counts/min. What is the strength of the source if 3000 counts are recorded in 1 min? What is the standard error of this measurement?

## REFERENCES


1 Masket, A. V., *Rev. Sci. Instr.* 28:191 (1957).
2 Ruffle, M. P., *Nucl. Instr. Meth.* 52:354 (1967).
3 Ruby, L., and Rechen, J. B., *Nucl. Instr. Meth.* 58:345 (1968).
4 Gotoh, H., and Yagi, H., *Nucl. Instr. Meth.* 96:485 (1971).
5 Gardner, R. P., and Verghese, K., *Nucl. Instr. Meth.* 93:163 (1971).
6 Verghese, K., Gardner, R. P., and Felder, R. M., *Nucl. Instr. Meth.* 101:391 (1972).
7 Williams, I. R., *Nucl. Instr. Meth.* 44:160 (1966).
8 Green, M. V., Aamodt, R. L., and Johnston, G. S., *Nucl. Instr. Meth.* 117:409 (1974).
9 Wielopolski, L., *Nucl. Instr. Meth.* 143:577 (1977).
10 Beam, G. B., Wielopolski, L., Gardner, R. P., and Verghese, K., *Nucl. Instr. Meth.* 154:501 (1978).
11 Tabata, T., Ito, R., and Okabe, S., *Nucl. Instr. Meth.* 94:509 (1971).
12 Kuzminikh, V. A., and Vorobiev, S. A., *Nucl. Instr. Meth.* 129:561 (1975).
13 Deruytter, A. J., *Nucl. Instr. Meth.* 15:164 (1962).
14 Walker, D. H., *Int. J. Appl. Rad. Isot.* 16:183 (1965).
15 Hutchinson, J. M. R., Nass, C. R., Walker, D. H., and Mann, W. B., *Int. J. Appl. Rad. Isot.* 19:517 (1968).
16 Waibel, E., *Nucl. Instr. Meth.* 74:236 (1969).
17 Waibel, E., *Nucl. Intr. Meth.* 86:29 (1970).
18 Waibel, E., *Nucl. Instr. Meth.* 131:133 (1975).
19 Bell, P. R., in K. Siegbahn (ed.), *Beta and Gamma-Ray Spectrometry*, Interscience Publishers, New York, 1955, Chap. 5.
20 Heath, R. L., "Scintillation Spectrometry–Gamma-Ray Spectrum Catalogue," IDO-16880-1 (1964).
21 Nakamura, T., *Nucl. Instr. Meth.* 86:163 (1970).


MEASUREMENT AND DETECTION OF RADIATION
N. TSOULFANIDIS (McGraw Hill, 1983)

# 9

# ■ introduction to spectroscopy

## 9.1 INTRODUCTION

Spectroscopy is the aspect of radiation measurements that deals with measuring the energy distribution of particles emitted by a radioactive source or produced by a nuclear reaction.

This introduction to spectroscopy is complemented by Chap. 11, which discusses methods of analysis of spectroscopic data, and Chaps. 12–14, which present details on spectroscopy of photons, charged particles, and neutrons. This chapter discussed the following broad subjects:

1 Definition of differential and integral spectra
2 Energy resolution of the detector
3 The function of a multichannel analyzer (MCA)

## 9.2 DEFINITION OF ENERGY SPECTRA

A particle energy spectrum is a function giving the distribution of particles in terms of their energy. There are two kinds of energy spectra, differential and integral.

The *differential energy spectrum*, the most commonly studied distribution, is also known as an energy spectrum. It is a function $n(E)$ with the following meaning:

$$n(E)\,dE = \text{number of particles with energies between } E \text{ and } E + dE$$

or $$n(E) = \text{number of particles per unit energy interval}$$

The quantity $n(E)\,dE$ is represented by the cross-hatched area of Fig. 9.1.

The *integral energy spectrum* is a function $N(E)$, where $N(E)$ is the number of particles with energy greater than or equal to $E$. The quantity $N(E)$ is represented by the hatched area of Fig. 9.1. The integral energy spectrum $N(E)$ and the differential energy spectrum $n(E)$ are related by

$$N(E) = \int_E^{\infty} n(E)\,dE \tag{9.1}$$

The two examples that follow illustrate the relationship between a differential spectrum and an integral spectrum.

*EXAMPLE 9.1* ■

Consider a monoenergetic source emitting particles with energy $E_0$. The differential energy spectrum $n(E)$ is shown in Fig. 9.2. Since there are no particles with energy

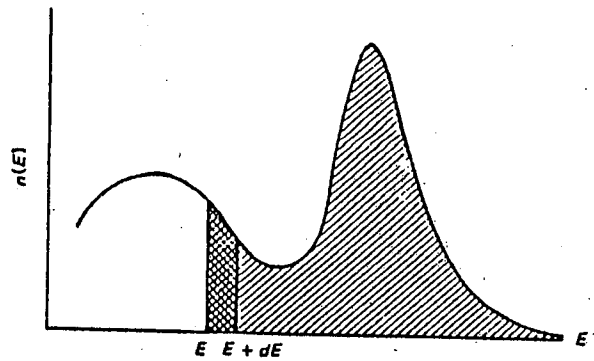


FIG. 9.1 A differential energy spectrum. The quantity $n(E)\,dE$ is equal to the number of particles between $E$ and $E + dE$ (cross-hatched area).

different than $E_0$, the value of $n(E)$ is equal to zero for any energy other than $E = E_0$.

The corresponding integral spectrum $N(E)$ is shown in Fig. 9.3. It indicates that there are no particles with $E > E_0$. Furthermore, the value of $N(E)$ is constant for $E < E_0$ since all the particles have energy $E_0$ and only those particles exist. In other words:

$N(E_0)$ = number of particles with energy greater than or equal to $E_0 = N(E_1)$

= number of particles with energies greater than or equal to $E_1$ (Fig. 9.3)

*EXAMPLE 9.2*

Consider the energy spectrum shown in Fig. 9.4. According to this spectrum there are 10 particles per MeV at 11, 12, and 13 MeV. The total number of particles is 30. The integral spectrum is shown in Fig. 9.5. Its value at different energies are:

$N(14) = 0$ no particles above $E = 14$ MeV

$N(13) = 10$ 10 particles at $E = 13$ MeV and above

$N(12) = 20$ 20 particles at $E = 12$ MeV and above

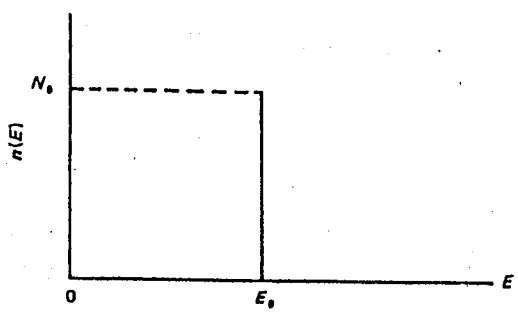


FIG. 9.2 A monoenergetic spectrum. All particles have energy $E_0$.



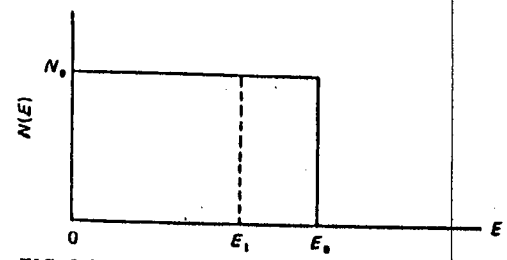


FIG. 9.3 The integral spectrum of a monoenergetic source.

$N(11) = 30$ 30 particles at $E = 11$ MeV and above

$N(10) = 30$ 30 particles at $E = 10$ MeV and above

$N(0) = 30$ 30 particles above $E = 0$

The determination of energy spectra is based on the measurement of pulse-height spectra, as shown in the following sections. Therefore, the definitions of differential and integral spectra given in this section in terms of energy could be expressed equivalently in terms of pulse height. The relationship between particle energy and pulse height is discussed in Sec. 9.5.

## 9.3 MEASUREMENT OF AN INTEGRAL SPECTRUM WITH A SINGLE-CHANNEL ANALYZER (SCA)

Measurement of an integral spectrum means to count all particles that have energy greater than or equal to a certain energy $E$ or, equivalently, to record all particles that produce pulse height greater than or equal to a certain pulse height $V$. A device is needed that can sort out pulses according to height. Such a device is a *single-channel analyzer* (SCA) operating as a discriminator (integral mode). If the discriminator is set at $V_0$ volts, all pulses with height less than $V_0$ will be rejected, while all pulses with heights above $V_0$ will be recorded. Therefore, a single discriminator can measure an integral energy spectrum. The measurement proceeds as follows.

Consider the differential pulse spectrum shown in Fig. 9.6 for which all the pulses have exactly the same height $V_0$. To record this spectrum, one starts with the

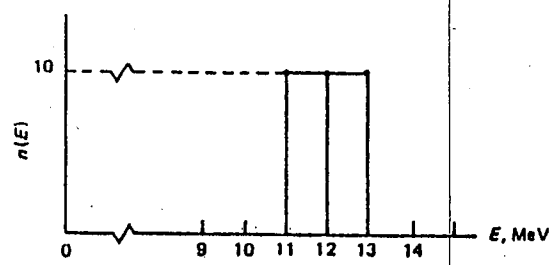


FIG. 9.4 The energy spectrum considered in Example 9.2.

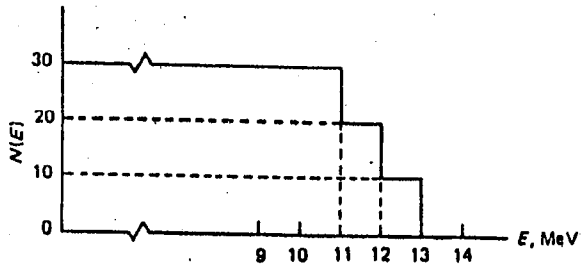


FIG. 9.5 The integral spectrum corresponding to that of Fig. 9.4.

discriminator threshold set very high (higher than $V_0$) and then lowers the threshold by a certain amount $\Delta V$ (or $\Delta E$) in successive steps. Table 9.1 shows the results of this measurement, where $N(V)$ is the number of pulses higher than or equal to $V$. A plot of these results is shown in Fig. 9.7.

## 9.4 MEASUREMENT OF A DIFFERENTIAL SPECTRUM WITH AN SCA

Measurement of a differential energy spectrum amounts to the determination of the number of particles within a certain energy interval $\Delta E$ for several values of energy; or, equivalently, it amounts to the determination of the number of pulses within a certain interval $\Delta V$, for several pulse heights. An SCA operating in the differential mode is the device that is used for such a measurement.

If the lower threshold of the SCA is set at $V_1$ (or $E_1$) and the window has a width $\Delta V$ (or $\Delta E$), then only pulses with height between $V_1$ and $V_1 + \Delta V$ are recorded. All pulses outside this range are rejected. To measure the pulse spectrum of Fig. 9.6, one starts by setting the lower threshold at $V_1$, where $V_1 > V_0$, with a certain window $\Delta V$ (e.g., $\Delta V = 0.1$ V) and then keeps lowering the lower threshold of the SCA. Table 9.2 shows the results of the measurement where $n(V)\,\Delta V$ is the number of pulses with height between $V$ and $V + \Delta V$. Figure 9.8 shows these results.

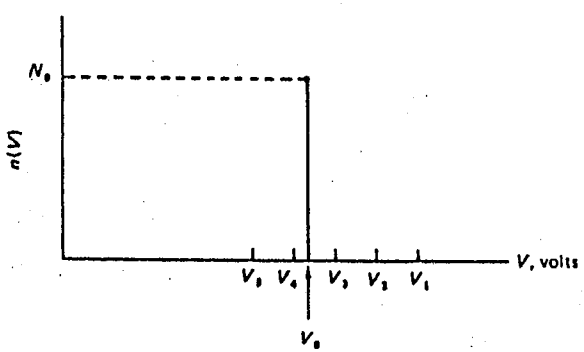


FIG. 9.6 A differential pulse spectrum consisting of pulses with the same height $V_0$.



TABLE 9.1 Measurement of Integral Spectrum

| Discriminator Threshold | $N(V)$ |
|---|---|
| $V_1 > V_0$ | 0 |
| $V_2$ | 0 |
| $V_3$ | 0 |
| $V_4 < V_0$ | $N_0$ |
| $V_5$ | $N_0$ |
| $V_6$ | $N_0$ |
| $V_i < V_0$ | $N_0$ |

It is assumed that the width is $\Delta V = V_i - V_{i+1}$, where $V_i$ are the successive settings of the lower threshold of the SCA. It is important to note that one never measures the value of $n(V)$, but only the product $n(V)\,\Delta V$.

## 9.5 THE RELATIONSHIP BETWEEN PULSE HEIGHT DISTRIBUTION AND ENERGY SPECTRUM

To determine the energy spectrum of particles emitted by a source, one measures, with the help of a detector and appropriate electronics, the pulse-height distribution produced by these particles. Fundamental requirements for the detector and the electronics are as follows:

1 The particle should deposit all its energy or a known constant fraction of it in the detector.
2 The voltage pulse produced by the detector should be proportional to the particle energy dissipated in it, or a known relationship should exist between energy dissipated and pulse height.
3 The electronic amplification should be the same for all pulse heights.

Since the relationship between pulse-height distribution and energy spectrum depends on these three requirements, it is important to discuss them in some detail.

Charged particles deposit all their energy in the detector, as long as their range is

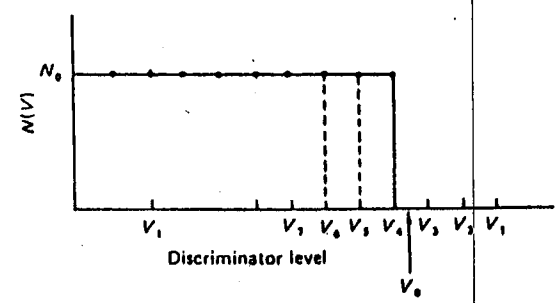


FIG. 9.7 The integral spectrum corresponding to the pulse spectrum of Fig. 9.6.

TABLE 9.2 Measurement of a Differential Spectrum

| SCA threshold | $n(V)\,\Delta V$ |
|---|---|
| $V_1 > V_0$ | 0 |
| $V_2$ | 0 |
| $V_3$ | 0 |
| $V_4 < V_0$ | $N_0$ |
| $V_5$ | 0 |
| $V_l < V_5$ | 0 |

smaller than the size of the detector. Gammas do not necessarily deposit all their energy in the detector, regardless of detector size. Neutrons are detected indirectly through other particles produced by nuclear reactions. The energy deposited in the detector depends not only on the energy of the neutron but also on the energy of the reaction products.

The events that transform the particle energy into a voltage pulse are statistical in nature. As a result, even if all the particles deposit exactly the same energy in the detector, the output pulses will not be the same but they will have a certain distribution.

The state of commercial electronics is such that the amplification is essentially the same for all pulse heights (see also Sec. 10.11).

As a result of incomplete energy deposition and the statistical nature of the events that take place in the detector, the shape of the pulse-height distribution is different from that of the source energy spectrum. In other words, two spectra are involved in every measurement:

1 The *source spectrum* is the energy spectrum of particles emitted by the source.
2 The *measured spectrum* is the measured pulse-height spectrum (or distribution).

Figure 9.9 shows as an example the source and the measured spectrum of a monoenergetic gamma source. The objective of the measurement is to obtain the spectrum of Fig. 9.9*a*, but the observer actually measures the distribution shown by Fig. 9.9*b*. The task of the observer is, therefore, to apply appropriate corrections to the measured spectrum to finally obtain the source spectrum.

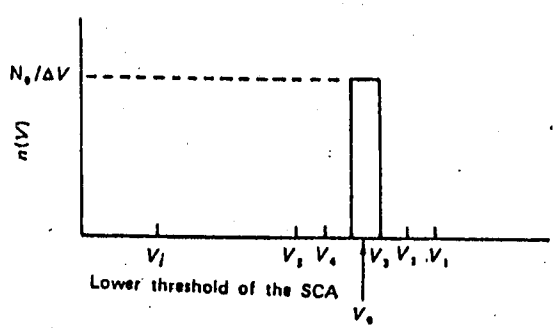


FIG. 9.8 A differential energy spectrum measured with an SCA.



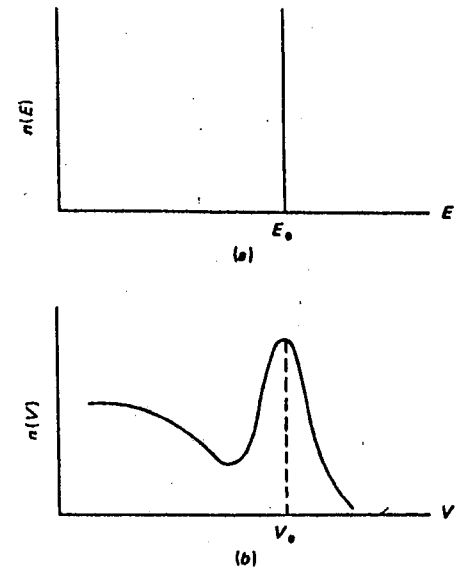


FIG. 9.9 (*a*) The source energy spectrum of a monoenergetic gamma source. (*b*) The pulse height distribution obtained with a NaI(Tl) scintillation counter.

## 9.6 ENERGY RESOLUTION

The performance of a detector used for energy measurements is characterized by the width of the pulse distribution of a monoenergetic source (Fig. 9.10). The *width*, measured at half of the maximum of the bell-shaped curve, is indicated by $\Gamma$ or by FWHM (full width half maximum). The ability of a detector to identify particles of different energies, called the *energy resolution*, is given either in terms of $\Gamma$ or in terms of the ratio $R(E_0)$, where

$$R(E_0) = \frac{\Gamma}{E_0} \tag{9.2}$$

The width $\Gamma$ is given in energy units, while the ratio $R(E_0)$ is given as a percentage. The three most important factors affecting the energy resolution are:

1 Statistical fluctuations in the number of charge carriers produced in the detector
2 Electronic noise in detector itself, the preamplifier, and the amplifier
3 Incomplete collection of the charge produced in the detector

### 9.6.1 The Effect of Statistical Fluctuations: The Fano Factor

To discuss the effect of the statistical fluctuations on energy resolution, consider a monoenergetic source of charged particles being detected by a silicon semiconductor detector. (The discussion would apply to a gas-filled counter as well.) The average

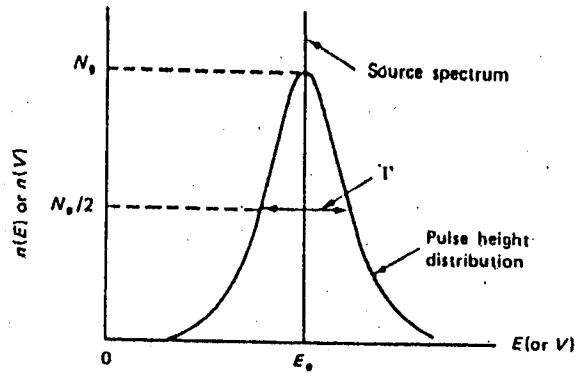


FIG. 9.10 The energy resolution of the detector is given by the width $\Gamma$ or the ratio $\Gamma/E_0$.

energy $w$ needed to produce one electron-hole pair in silicon is 3.66 eV, although the energy gap ($E_g$) is 1.1 eV. This difference between $w$ and $E_g$ shows that part of the energy of the incident particles is dissipated into processes that do not generate charge carriers. Any process that consumes energy without producing electron-hole pairs is, of course, useless to the generation of the detector signal. If the energy deposited in the detector is $E$, the average number of charge carriers is $E/w$. If the process of electron-hole generation were purely statistical, Poisson statistics would apply and the standard deviation of the number of pairs would be

$$\sigma = \sqrt{\frac{E}{w}} \tag{9.3}$$

Experience has shown that the fluctuations are smaller than what Eq. 9.3 gives. The observed statistical fluctuations are expressed in terms of the *Fano factor* $F$,[1] where

$$F = \frac{(\text{standard deviation of the number of pairs produced})^2}{\text{number of pairs produced}}$$

or, using Eq. 9.3,

$$\sigma = \sqrt{\frac{FE}{w}} \tag{9.4}$$

The two extreme values of $F$ are 0 and 1.

$F = 0$ means that there are no statistical fluctuations in the number of pairs produced. That would be the case if all the energy was used for production of charge carriers. $F = 1$ means that the number of pairs produced is governed by Poisson statistics.

Fano factors have been calculated and also measured.[2-5] For semiconductor detectors, $F$ values as low as 0.06 have been reported.[6] For gas-filled counters, reported $F$ values lie between 0.2 and 0.5. Values of $F < 1$ mean that the generation of electron-hole pairs does not exactly follow Poisson statistics. Since Poisson statistics applies to outcomes that are independent, it seems that the ionization events in a counter are interdependent.



The width $\Gamma$ of a Gaussian distribution, such as that shown in Fig. 9.10, is related to the standard deviation $\sigma$ by

$$\Gamma_f = 2\sqrt{2 \ln 2}\, w\sigma \approx 2.355 w\sigma \tag{9.5}$$

Combining Eqs. 9.4 and 9.5,

$$\Gamma_f = 2\sqrt{2(\ln 2) wFE} \tag{9.6}$$

Equation 9.5 shows that the width $\Gamma_f$, which is due to the statistical fluctuations, is roughtly proportional to the square root of the energy (the Fano factor is a weak function of energy).

To compare the contribution of the statistical fluctuations to the resolution of different types of detectors at a certain energy, one can use Eqs. 9.2 and 9.6 and write for detectors 1 and 2

$$\frac{R_1}{R_2} = \frac{\Gamma_1/E}{\Gamma_2/E} = \sqrt{\frac{w_1 F_1}{w_2 F_2}} \tag{9.7}$$

It can be seen from Eq. 9.7 that the resolution is better for the detector with the smaller average energy needed for the creation of a charge carrier pair (and smaller Fano factor). Thus, the energy resolution of a semiconductor detector ($w = 3$ eV, $F < 0.1$) should be expected to be much better than the resolution of a gas-filled counter ($w \approx 30$ eV, $F \approx 0.2$), and indeed it is (see Chaps. 12 and 13).

### 9.6.2 The Effect of Electronic Noise on Energy Resolution

The electronic noise consists of a small voltage variation around the zero line (Fig. 9.11), with average voltage $\bar{v}_n \neq 0$. To see the effect of the noise on the energy resolution, consider pulses of constant height $V$. In the absence of noise, the FWHM of the distribution of these pulses is zero. If noise is present, the pulses will be superimposed on the noise with the results that the pulses are not of equal height any more (Fig. 9.12), and that the pulses form a Gaussian distribution centered at $V$ and having a width equal to $\Gamma_n = 2\sqrt{2 \ln 2}\, \sigma_n$. The width $\Gamma_n$ is due to the noise only and has nothing to do with statistical effects in the detector.

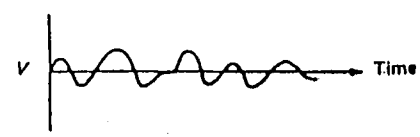


FIG. 9.11 The electronic noise.

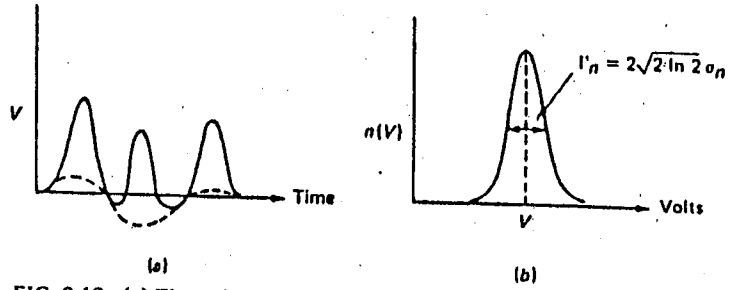


FIG. 9.12 (*a*) The pulses are superimposed on the noise, as a result of which (*b*) they show a distribution with a width which depends on the standard deviation of the noise.

The *signal-to-noise ratio* is frequently the quantity used to indicate the magnitude of the noise. It is defined by:

$$\text{Signal-to-noise ratio} = \frac{\text{mean pulse height}}{\text{noise standard deviation}} = \frac{V}{\sigma_n}$$

Or, one can write

$$\frac{V}{\sigma_n} = 2\sqrt{2 \ln 2}\,\frac{V}{\Gamma_n} = \frac{2\sqrt{2 \ln 2}}{R} \tag{9.8}$$

where $R$ is given by Eq. 9.2. This last equation may be rewritten as

$$R = \frac{2\sqrt{2 \ln 2}}{V/\sigma_n} \tag{9.8a}$$

to show that the higher the signal-to-noise ratio is, the better the resolution becomes (other things being equal, of course).

### 9.6.3 The Effect of Incomplete Charge Collection

The effect of incomplete charge collection in gas counters is small compared to the effect of the statistical fluctuations. In semiconductor detectors, incomplete charge collection is due to trapping of carriers. The amount of charge trapped is approximately proportional to the energy deposited in the detector, which in turn is proportional to the energy of the incident particles.[7] For this reason, the resolution is affected by trapping effects more at high energy than at low energy. As discussed in Chap. 7, trapping effects depend on the material of which the detector is made and on radiation damage suffered by the semiconductor. Usually, the effect of incomplete charge collection is included in the statistical fluctuations.

### 9.6.4 The Total Width Γ

The total width Γ (or the total energy resolution) is obtained by adding in quadrature the contributions from the statistical effects ($\Gamma_f$) and from the noise and incomplete charge collection ($\Gamma_n$). Thus,



$$\Gamma = \sqrt{\Gamma_f^2 + \Gamma_n^2} \tag{9.9}$$

For gas and scintillator counters, the main contribution comes from the statistical fluctuations. For semiconductor detectors at low energies, measurements have shown that $\Gamma_n \gtrsim \Gamma_f$. At higher energies this is reversed, since $\Gamma_n$ is essentially independent of energy while $\Gamma_f$ increases with it (see Eq. 9.6).

## 9.7 DETERMINATION OF THE ENERGY RESOLUTION—THE RESPONSE FUNCTION

Depending on the type and energy of the incident particle and the type of the detector, a monoenergetic source produces a pulse-height distribution that may be a Gaussian (Fig. 9.10) or a more complicated function (Fig. 9.9). In either case, one concludes that although all the particles start at the source with the same energy, there is a probability that they may be recorded within a range of energies. That probability is given by the *response function* or *energy resolution function* $R(E, E')$ of the detection system, defined as:

$R(E, E')\,dE$ = probability that a particle emitted by the source with energy $E'$ will be recorded with energy between $E$ and $E + dE$

One measures, of course, a pulse-height distribution, but the energy calibration of the system provides a one-to-one correspondence between energy and pulse height. If one defines

$S(E)\,dE$ = source spectrum = number of particles emitted by the source with energy between $E$ and $E + dE$

and

$M(E)\,dE$ = measured spectrum = number of particles recorded as having energy between $E$ and $E + dE$

then the three functions $R(E, E')$, $S(E)$, and $M(E)$ are related by

$$M(E) = \int_0^\infty R(E, E')S(E')\,dE' \tag{9.10}$$

Equation 9.10 is an integral equation with the source spectrum $S(E)$ being the unknown. The procedure by which $S(E)$ is obtained, after $R(E, E')$ and $M(E)$ have been determined, is called *unfolding* of the measured spectrum. Methods of unfolding are discussed in Chaps. 11–14.

To determine the response function of a detection system at energy $E$, the energy spectrum of a monoenergetic source emitting particles with that energy is recorded. Since the resolution changes with energy, the measurement is repeated using several sources spanning the energy range of interest. The response function can also be calculated, as shown in Chap. 12–14. Figure 9-13 shows response functions for several commonly encountered cases.

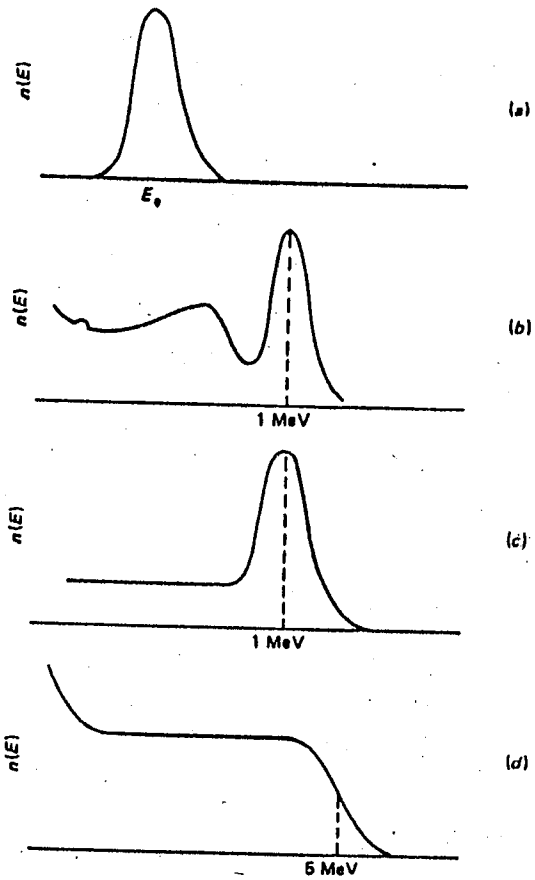


FIG. 9.13 Four examples of response functions. (*a*) 5-MeV Alpha particles detected by a silicon surface barirer detector (Chap. 13), or 20-keV x-rays detected by a Si(Li) reactor (Chap. 12). (*b*) 1-MeV Gamma ray detected by a NaI(Tl) crystal (Chap. 12). (*c*) 1-MeV Electrons detected by a plastic scintillator (Chap. 13). (*d*) 5-MeV Neutrons detected by an NE-213 organic scintillator (Chap. 14).

## 9.8 THE IMPORTANCE OF GOOD ENERGY RESOLUTION

The importance of good energy resolution becomes obvious if the energy spectrum to be measured consists of several energies. Consider as an example the source spectrum of Fig. 9.14, consisting of two energies $E_1$ and $E_2$. Assume that this spectrum is measured with a system having energy resolution equal to $\Gamma$,† and examine the following cases.

†$\Gamma$ may be different at $E_1$ and $E_2$. However, the difference is very small since $E_1$ and $E_2$ are close. For the present discussion, the same $\Gamma$ will be used at $E_1$ and $E_2$.



CASE I: $E_2 - E_1 > 2\Gamma$

The measured spectrum is shown in Fig. 9.15 for this case. The system can *resolve* the two peaks—i.e., the two peaks can be identified as two separate energies.

CASE II: $E_2 - E_1 = 2\Gamma$

This case is shown in Fig. 9.16. The peaks can still be resolved.

CASE III: $E_2 - E_1 = \Gamma$

This case is shown in Fig. 9.17. The solid line shows how the measured spectrum will look as the sum of the two peaks (dashed lines).

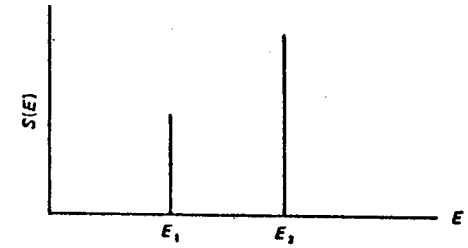


FIG. 9.14 Source spectrum consisting of two distinct energies.

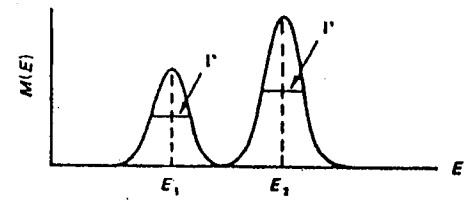


FIG. 9.15 Measured spectrum for Case I: $2\Gamma < E_2 - E_1$.

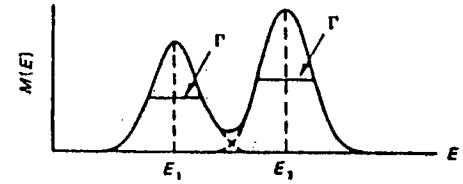


FIG. 9.16 Measured spectrum for case II: $2\Gamma = E_2 - E_1$.

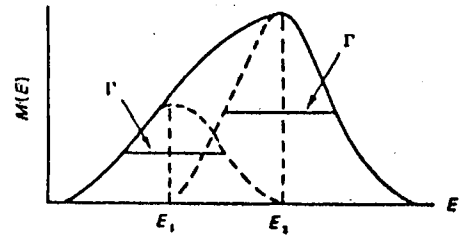


FIG. 9.17 Measured spectrum for Case III: $\Gamma = E_2 - E_1$.

It is obvious that it is difficult to identify two distinct peaks if $E_2 - E_1 = \Gamma$, and the situation will be worse if $E_2 - E_1 < \Gamma$.

The three cases examined above intend to show how important good energy resolution is for the measurement of spectra with many energy peaks. If the response function of the detector is not known and the measured spectrum shows no well-identified peaks, the following criterion is used for the energy resolution required to identify the peaks of about equal magnitude:

> To be able to resolve two energy peaks at $E_1$ and $E_2$, the resolution of the system should be such that $\Gamma < |E_1 - E_2|$.

## 9.9 BRIEF DESCRIPTION OF A MULTICHANNEL ANALYZER (MCA)

To measure an energy spectrum of a radioactive source means to record the pulse-height distribution produced by the particles emitted from the source, which is achieved with the use of an instrument called the multichannel analyzer (MCA). Multichannel analyzers are used in either of two different modes: the *pulse-height analysis* (PHA) mode or the *multichannel scaling* (MCS) mode.

The PHA mode is the tradiational function of a MCA and is used to sort out incoming pulses according to their height and store the number of pulses of a particular height in a corresponding address of the MCA memory called the *channel number*.

The MCS mode is used to count events as a function of time. The individual channels of the memory count all incoming pulses for a preset time width $\Delta t$. After time $\Delta t$, the counting operation is switched automatically to the next channel in the memory, thus producing in the end a time sequence of the radiation being detected. For example, if the radiation source is a short-lived isotope, the MCS mode will provide the exponential decay curve that can be used for the measurement of the half-life of this isotope.

In the PHA mode, an MCA performs the function of a series of SCAs placed adjacent to one another. When only one SCA with width $\Delta E$ is used, the experimenter has to sweep the spectrum by moving the lower threshold of the SCA manually (see Sec. 9.4). On the other hand, if one had many SCAs, all counting simultaneously, the whole spectrum would be recorded simultaneously. This is exactly what the MCA does, although its principle of operation is not based on a series of SCAs.

Figure 9.18 shows a simplified block diagram of a MCA. In the PHA mode, the

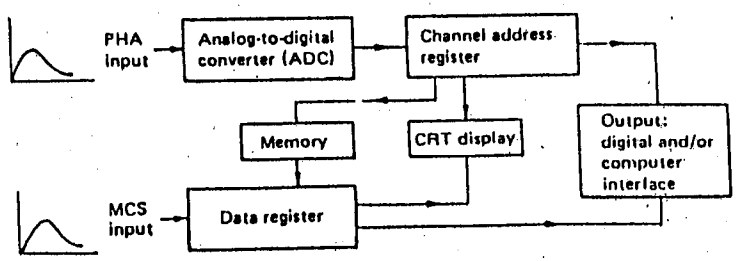


FIG. 9.18 A simplified block diagram of an MCA.



incoming pulse enters into a unit called the *analog-to-digital converter* (ADC). The ADC *digitizes* the pulse amplitude: it produces a number proportional to the height of the pulse, a number which determines the channel where the pulse will be stored. The size of the ADC, given in terms of channels, defines the absolute resolution of the system. Actually, the ADC determines the number of discrete parts into which the pulse height can be subdivided. Commercial ADCs have at the present time a size up to 8192 channels, with the full scale adjustable in steps of 256, 512, 1024, etc., channels.

The number of discrete parts (channels) into which the input pulse range (0 to +10 V) is divided is called the *conversion gain*. The conversion gain is set by a step-wise control knob located on the front of the instrument. As an example, if the conversion gain is set at 2048 channels, it means that the maximum pulse height (10 V) is divided into that many parts. Therefore, the resolution of the MCA at this setting is:

$$10\ \text{V}/2048 = 4.88\ \text{mV/channel}$$

More details about the operation and characteristics of ADCs are given in Sec. 10.12.

The memory of the MCA is a data-storage unit arranged in a series of channels. Every channel is capable of storing up to $2^{20} - 1$ data (pulses), in most cases. Commercial MCAs have memories with up to 8192 channels. Normally, the MCA provides for selection and use of the full memory, of only half of it, or of one-fourth of it. Transfer of data from one fraction of the memory to another is also possible.

In the PHA mode, the first channel of the region used is called *channel zero* and records, in almost all late model MCAs, the live time of the analysis, in seconds. If the full memory or the first half or first quarter of the memory is used, channel zero is the address 0000. If the second half of a 4096 memory is used, channel zero is address 2048; if the second quarter is used, channel zero is address 1024; and so on.

How does one determine the size of the MCA memory needed for a specific experiment? The decision is made based on the requirements for the PHA mode. One equation frequently used is

$$\text{Number of channels} = h\,\frac{\text{energy range of interest (keV)}}{\Gamma\ \text{(keV)}} \tag{9.12}$$

where $\Gamma$ is the FWHM of the detector used. The factor $h$ is equal to the number of channels at or above the FWHM of the peak. Its value is between 3 and 5.

As an example, assume that the energy range of interest is 0 to 2.0 MeV and consider a NaI(Tl) and a Ge(Li) detector. The resolution of the NaI(Tl) detector is about 50 keV. Therefore, the minimum number of channels is ($h = 5$)

$$5\left(\frac{2000}{50}\right) \approx 200\ \text{channels}$$

The resolution of a Ge(Li) detector is about 2 keV. Now, the number of channels is

$$5\left(\frac{2000}{2}\right) \approx 5000\ \text{channels}$$

The user should remember that the ADC, not the memory, determines the absolute resolution of an MCA. An MCA with an ADC of 1000 channels and a memory of 2000 channels has an actual resolution of only 1000 channels.

The major disadvantage of every MCA is the dependence of its dead time on the channel where the pulse is stored. The equation for dead time is of the form

$$\tau = a_1 + a_2 C + a_3 \tag{9.13}$$

where $a_1$, $a_2$, and $a_3$ are constants given by the manufacturers and $C$ is the channel number. Typical values are $a_1 \approx 2.5$ μs, $a_2 = 0.01$ to 0.02 μs/channel and $a_3 = 0$ to 7 μs. Thus, if a pulse is stored in channel 2000, the dead time is

$$\tau \approx 2.5 + 0.02(2000) + 7 \approx 47\ \mu s$$

The dead-time correction should be applied separately for every channel, using the method shown in Sec. 2.20.

Commercial MCAs have a meter that shows, during counting, the percent of dead time. They also have timers that determine the counting period in *live time* or *clock time*. In clock time mode, the counting continues for as long as the clock is set up. In live time mode, an automatic correction for dead time is performed. In this case, the percent dead time indication can be used to determine the approximate amount of actual time the counting will take. For example, if the clock is set to count for 5 min (in live mode) and the dead time indicator shows 25 percent, the approximate actual time of this measurement is going to be,

$$\text{Actual time} = \frac{\text{live time}}{1 - (\text{dead time fraction})} = \frac{300\ \text{s}}{1 - 0.25} = 400\ \text{s}$$

Modern MCAs can do much more than store the number of pulses in the memory. They are, essentially, hard-wired minicomputers that may be able to integrate the area under a spectrum, find the energy of a peak and, in some cases, select the isotope that emits a photon of certain energy. Also marketed today are MCAs that are connected with minicomputers of their own, have their own library of programs, and can analyze quantitatively any spectrum. Most of the controls are on a push-button console located in front of a large cathode-ray tube.

## 9.10 CALIBRATION OF A MULTICHANNEL ANALYZER

The calibration of an MCA follows these steps:

1. *Determination of range of energies involved.* Assume this is $0 \leq E \leq E_m$ (MeV).

2. *Determination of preamplifier-amplifier setting.* Using a source which emits particles of known energy, one observes the signal generated on the screen of the oscilloscope. It should be kept in mind that the maximum possible signal at the output of the amplifier is 10 V. In energy spectrum measurements, one should try to stay in the range 0–9 V.



Assume that the particle energy $E_1$ results in pulse height $V_1$. Is this amplification proper for obtaining a pulse height $V_m \leq 10$ V for energy $E_m$? To find this out, the observer should use the fact that pulse height and particle energy are proportional. Therefore:

$$\frac{V_m}{E_m} = \frac{V_1}{E_1} \rightarrow V_m = \frac{E_m}{E_1} V_1$$

If $V_m < 10$ V, then the amplification setting is proper. If $V_m > 10$ V, the amplification should be reduced. (If $V_m < 2$ V, amplification should be increased. It is good practice, but not necessary, to use the full range of allowed voltage pulses.) The maximum pulse $V_m$ can be changed by changing the amplifier setting.

3. *Determination of MCA settings.* One first decides the part of the MCA memory to be used. Assume that the MCA has a 1024-channel memory and it has been decided to use 256 channels, one-fourth of the memory. Also assume that a spectrum of a known source with energy $E_1$ is recorded and that the peak is registered in channel $C_1$. Will the energy $E_m$ be registered in $C_m < 256$, or will it be out of scale?

The channel number and energy are almost proportional,† i.e., $E_i \sim C_i$. Therefore

$$\frac{C_m}{E_m} \approx \frac{C_1}{E_1} \rightarrow C_m \approx \frac{E_m}{E_1} C_1$$

If $C_m \leq 256$, the setting is proper and may be used. If $C_m > 256$, a new setting should be employed. This can be done in one of two ways or a combination of the two:

1. The fraction of the memory selected may be changed. One may use 526 channels of 1024, instead of 256.
2. The conversion gain may be changed. In the example discussed here, if a peak is recorded in channel 300 with conversion gain of 1024, that same peak will be recorded in channel 150 if the conversion gain is switched to 512.

There are analyzer models that do not allow change of conversion gain. For such an MCA, if $C_m$ is greater than the total memory of the instrument, one should return to step 2 and decrease $V_m$ by reducing the gain of the amplifier.

4. *Determination of the energy-channel relationship.* Calibration of the MCA means finding the expression that relates particle energy to the channel where a particular energy is stored. That equation is written in the form

$$E = a_1 + a_2 C + a_3 C^2 \tag{9.14}$$

where $C$ = channel number and $a_1, a_2, a_3, \ldots$ are constants.

The constants $a_1, a_2, a_3, \ldots$ are determined by recording spectra of sources with known energy. In principle, one needs as many energies as there are constants.

†The correction equation is $E = a + bC$, but $a$ is small and for this argument it may be neglected; proper evaluation of $a$ and $b$ is given in step 4 of the calibration procedure.

In practice, a large number of sources is recorded with energies covering the whole range of interest and the constants are then determined by a least-squares fitting process (see Chap. 11).

Most detection systems are essentially linear, which means that Eq. 9.14 takes the form

$$E = a_1 + a_2 C \tag{9.15}$$

*EXAMPLE 9.3*

Obtain the calibration constants for an MCA based on the spectrum shown in Fig. 9.19. The peaks correspond to the following three energies:

$E_1 = 0.662$ MeV $\quad C_1 = 160$

$E_2 = 1.173$ MeV $\quad C_2 = 282.5$

$E_3 = 1.332$ MeV $\quad C_3 = 320$

*ANSWER*

Plotting energy versus channel on linear graph paper, one obtains the line shown in Fig. 9.20, which indicates that the linear equation, Eq. 9.15, applies, and one can determine the constants $a_1$ and $a_2$ from the slope and the zero intercept of the straight line. From Fig. 9.19, the value of $a_2$ is

$$a_2 = \frac{950 - 400}{230 - 97.5} = 4.15 \text{ keV/channel}$$

The constant $a_1$ is equal to the zero-intercept of the line.† In the present case, it is almost zero. Based on these results, the calibration equation of this MCA is $E = 4.15C$.

5. *Calculation of the energy resolution.* By definition, the energy resolution is $R = \Gamma/E$, where $\Gamma$ is the FWHM of the peak of energy $E$. Therefore, using Eq. 9.15,

$$R = \frac{\Gamma}{E} = \frac{(a_1 + a_2 C_R) - (a_1 - a_2 C_L)}{E} = \frac{a_2(C_R - C_L)}{E} \tag{9.16}$$

†Most commercial MCAs have a hand-screw adjustment that makes $a_1$ equal to zero.

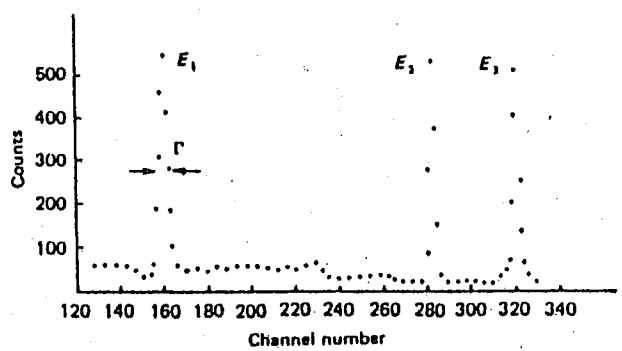


FIG. 9.19 A gamma spectrum used for calibration of an MCA.



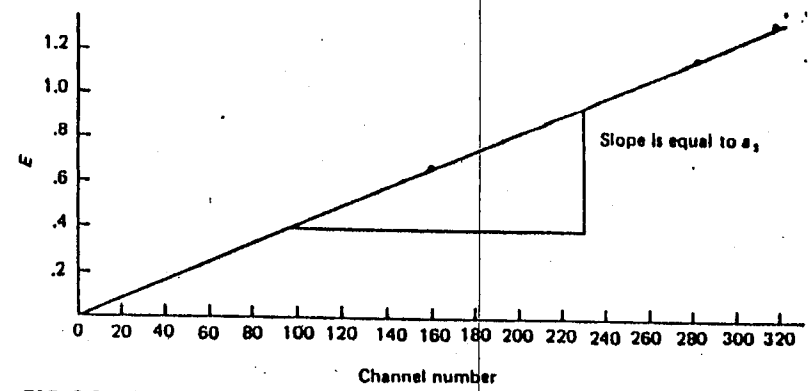


FIG. 9.20 Plot of energy versus channel number. In this case, the relationship is linear.

where $C_R$ and $C_L$ are the channel numbers on either side of the peak at half of its maximum. If $a_1$ is zero, the resolution is given by

$$R = \frac{a_2(C_R - C_L)}{a_2 C_{\text{peak}}} = \frac{C_R - C_L}{C_{\text{peak}}} \tag{9.17}$$

For peak $E_1$ (Fig. 9.18),

$$C_L = 158 \qquad C_{\text{peak}} = 160 \qquad C_R = 162$$

Therefore

$$R = \frac{162 - 158}{160} = 2.5\%$$

or $\quad \Gamma = a_2(C_R - C_L) = 4.15(4) = 16.6$ keV

## PROBLEMS

9.1 Sketch the integral spectrum for the diffferential spectrum shown in the figure below.

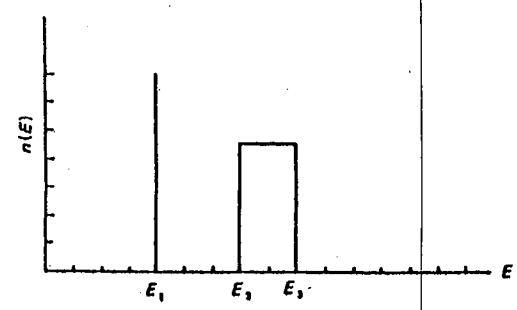

9.2 Sketch the differential energy spectrum for the integral spectrum shown in the figure below.

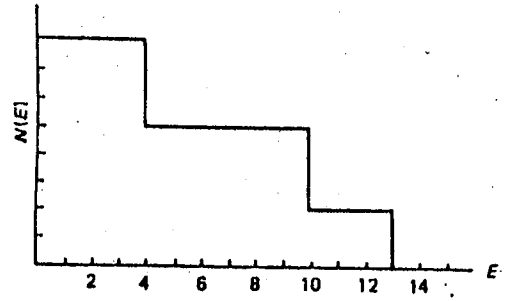


9.3 Sketch the integral spectrum for the differential spectrum shown in the figure below.

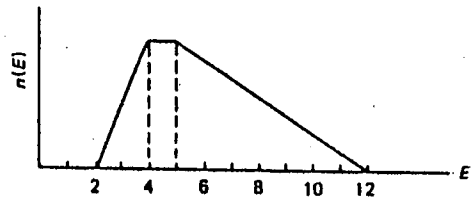


9.4 If the energy resolution of a NaI(Tl) scintillator system is 11 percent at 600 keV, what is the width Γ of a peak at that energy?

9.5 What is the maximum energy resolution ncesssary to resolve two peaks at 720 keV and 755 keV?

9.6 Prove that if a detection system is known to be linear the calibration constants are given by

$$a_1 = \frac{E_2 C_1 - E_1 C_2}{C_1 - C_2} \qquad a_2 = \frac{E_1 - E_2}{C_1 - C_2}$$

where $E_1$ and $E_2$ are two energies recorded in channels $C_1$ and $C_2$, respectively.

9.7 Shown in the figure below is the spectrum of $^{22}$Na, with its decay scheme. Determine the calibration constants of the MCA which recorded this spectrum, based on the two peaks of the $^{22}$Na spectrum.

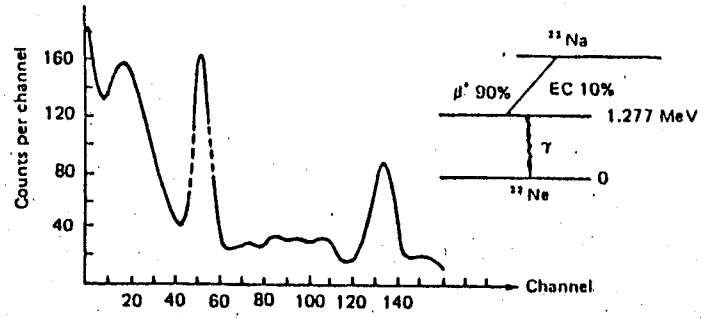




9.8 In Prob. 9.7, the channel number cannot be read exactly. What is the uncertainty of the calibration constants $a_1$ and $a_2$ if the uncertainty in reading the channel is one channel for either peak?

9.9 Assume that the energy resolution of a scintillation counter is 9 percent and that of a semiconductor detector is 1 percent at energies around 900 keV. If a source emits gammas at 0.870 MeV and 0.980 MeV, which of these peaks can be resolved with a scintillator and which ones with a semiconductor detector?

9.10 Consider the two peaks shown in the accompanying figure. How does the peak at $E_2$ affect the width of the peak at $E_1$ and vice versa? What is the width Γ for either peak?

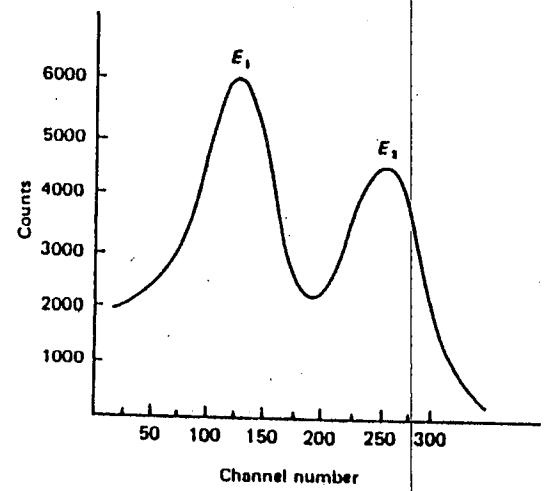


## REFERENCES


1 Fano, U., *Phys. Rev.* 72:26 (1947).
2 van Roosbroeck, W., *Phys. Rev.* 139A:1702 (1965).
3 Goulding, F. S., *Nucl. Instr. Meth.* 43:1 (1966).
4 Mann, H. M., Bilger, H. R., and Sherman, I. S., *IEEE* NS-13(3):352 (1966).
5 Deshpande, R. Y., *Nucl. Instr. Meth.* 57:125 (1967).
6 Pehl, R. H., and Goulding, F. S., *Nucl. Instr. Meth.* 81:329 (1970).
7 Ewan, G. T., *Nucl. Instr. Meth.* 162:75 (1979).

24 HOURS ACTIVATION

NUCLEAR ENGINEERING LABORATORY
N.E. E4710

EXPERIMENT #5
ACTIVATION ANALYSIS BY MEASUREMENT
OF GAMMA RAYS

---

OBJECTIVE:

The purpose of this experiment is to introduce the student to activation analysis. Although activation can be aomplished by particles other than neutrons, this experiment involves activation by thermalized neutrons and subsequent analysis by observing the gamma ray emission of the radioisotope formed.

EQUIPMENT:

Neutron Howitzer with PuBe neutron sources
Indium Foils
Model 1024D Multichannel Analyser
Scintillation Detector
GM Counter
ORTEC or RIDL associated equipment

DISCUSSION:

When a material is bombarded or irradiated by the nuclear particles produced from a suitable source, some of the atoms present in the samples will interact with the bombarding particles. These atoms may be converted into different isotopes of the same element, or isotopes of different elements depending on the nature of the bombarding particles. In many cases, the isotopes produced are radioactive and termed radioisotopes. If the redioactivity which is induced in one isotope of a mixed material can be distinguished from all other radioactivities arising at the same time, or originally present, then the amount of this induced radioactivity is a measure of the parent isotope and therefore of the parent element, present in the original material.

It can be shown that the weight of the element present is:

$$W = \frac{M A e^{-\lambda t}}{o\ v\ f\ (1 - e^{-\lambda t})\ 6.02 \times 10^{23}}$$

where
A = disintegrations/second
M = atomic weight
t = radiation time
T = time after bombardment analysis is started
f = fractional abundance of the specific isotope.
v = capture cross section
0 = neutron flux
> = decay constant

START HERE

Then, in principle, all factors are known. In practice, however, v is not known with sufficient accuracy, 0 can not be determined accurately and sometimes it is not easy to determine A. Consequently, a comparison procedure is invariably used, and the amount of activity from the sample is compared with that from a standard amount
[ Omega: Your prime-time CPU time limit is exceeded. ]
of element being determined. Thus, weight of element in sample = Cx/Cs [weight of element in standard]. Where Cx is the observed counting rate of the sample, and Cs that of the standard measured under comparable condition.

Use This Technique

In order to determine the radioactivity assoc
[ Omega: You have one minute to save your work and logout. ]
iated with a particular gamma ray energy, it is necessary to measure the number of counts in the photopeak. Under ideal conditions, this can be done in one of three ways: (1)by measuring the heighth of the photopeak, (2) by measuring the number of counts in the channel corresponding to the center of the photopeak, or (3) by measuring the area under the photopeak. This procedure is left to the discretion of the experimenter.

PROCEDURE:

In this experiment, $MnSO_4.H_2O$, $Na_2CO_3$ and a mixture of $MnSO_4.H_2O$ and $Na_2CO_3$ are exposed to thermal neutrons (in the neutron howitzer) for at least 24 hours. Thin indium foils are attached to each capsule of the various compounds. Standards are make of $MnSO_4.H_2O$ and plus its indium foil and of the $Na_2CO_3$ plus its indium foils. (This is done by printing out the spectrum of each of the standards and thier respective foils and calculating the radioactivity. By normalizing the fluxes of the two standards, it is then possible to determine the amount of $MnSO_4.H_2O$ and $NaCO_3$ in the unknown solution by using the two standards. (note record the exact time each count is performed)

REPORT:

Determine the weight of $MnSO_4.H_2O$ and $Na_2CO_3$ in the unknown capsule. Remember to consider self-absorbtion. Show all analysis in your report. Explain the experimental proedure and equipment used in this experiment. In this experiment, $MnSo_4,H_2O$ and $Na_2Co_3$ have been exposed to thermal neutrons. Why only Mn and
[ Omega: Logging you out now. Come back after prime time. ]
Na isotopes were detected.

REFERENCES:

1) Kaplan, Irving - "Nuclear

NUCLEAR ENGINEERING LAVORATORY
N.E. E4710

# EXPERIMENT # 4
# CHARACTERISTICS OF A MULTICHANNEL ANALYZER

---

OBJECTIVE:

To acquaint the student with the characteristics, advantages, and uses of a multichannel analyzer.

EQUIPMENT:

Model 1024D Multichannel Analyzer (MCA)
Sodium iodide scintillation detector and associated counting equipment
Atomic precision pulse generator
High voltage supply
Various gamma sources

PROCEDURE:

Note: Review over the handout for the operation for the MCA before beginning this procedure.

1. Connect the amplifier output to the DIRECT INPUT of the analyzer and store the Cs-137 spectrum for an arbitrary time. Remove the source and store background in the negative mode for the same amount of time. Is the background count necessary?

2. The amplifier gain switch controls the amplification of the pulses entering the analyser. If the amplifier gain is raised by a factor of 2, the energy per channels calibration is lowered by a factor of 2. Check this calibration by storing Cs-137 at different amplifier gain settings. Plot the channel corresponding to the photo-peak of Cs-137 versus gain setting and discuss.

3. Use fine gain in conjunction with the high voltage to adjust calibration of the instrument to be Mev/channnel = 2 kev (i.e. photo peak of Cs-137 (662 kev) must be seen at channel 331). Under no circumstances should the voltage be raised above 1000 Volts. Store Co-60 and determine the channels corresponding to the photopeaks of this source. Plot channel number versus photopeak energy and verify linearity of the MCA. You may use region of interest sectioning to print out only the channels around the photopeak.

4. Use another gamma ray source Ba-137 and determine the

energy of the photopeak. Check your result with literature.

5. Check the linearity of the analyzer with the Atomic Pulse generator (e.g., the number of channels between several pulses which differ in equal increments of voltage should be the same). Set the amplifier to minimum gain and hook up the direct ouput of the generator to the input of the amplifier. Analyze the output of the generator long enough to get a good peak a each setting of the pulse height. Stop the analyse between movements of the pulse heighth dial. Try to get readings over the entire range of the analyzer. Record all of the pulse height dial settings and get a print out of the spectrum. Determine if the MCA is linear over its entire range.

QUESTIONS:

1. In what ways is a multichannel analyzer more versatile than a single channel analyzer? Name several situations in which a multichannel analyzer could be used, but a single channel analyzer could not.

2. If the MCA had the ability to store several spectrums, how would this be helpful.

3. What is the effect of the amplifier gain and high voltage on analyser output.

REPORT:

This report is more qualitative than most of the others. The student should report characteristics of the analyzer not covered in the manual which he thinks are important.

REFERENCES:

1. MCA manual

11.7 Prove that the result of folding an exponential function $e^{-aE}$ with a Gaussian is

$$M(E) = e^{a^2\sigma^2/2}e^{-aE}$$

11.8 What is the measured spectrum $M(E)$ if the detector response is a step function of the form $R(E, E') = C(E')/E'$ and the source emits two types of particles at energy $E_1$ and $E_2$?

11.9 What is the measured spectrum $M(E)$ if the detector response is a step function, as in Prob. 11.8, and the source spectrum is

$$S(E) = \frac{S_0}{E_2 - E_1} \qquad E_1 < E < E_2$$

and is zero otherwise.

11.10 The following data represent results of counting an energy peak. How does the FWHM of the peak change if one applies (a) three-point zeroth-order smoothing and (b) five-point second-order smoothing?

| Channel | Counts | Channel | Counts |
|---|---|---|---|
| 10 | 12 | 17 | 34 |
| 11 | 10 | 18 | 26 |
| 12 | 14 | 19 | 18 |
| 13 | 14 | 20 | 10 |
| 14 | 24 | 21 | 12 |
| 15 | 30 | 22 | 9 |
| 16 | 40 | | |

## BIBLIOGRAPHY

Abramowitz, M., and Stegan, I. A. (eds.), *Handbook of Mathematical Functions*, National Bureau of Standards, Applied Mathematics Series, 55, June 1964.

Bevington, P. R., *Data Reduction and Error Analysis for the Physical Sciences*, McGraw-Hill, New York, 1969.

Hildebrand, F. B., *Introduction to Numerical Analysis*, McGraw-Hill, New York, 1956.

Householder, A. S., *Principles of Numerical Analysis*, McGraw-Hill, New York, 1953.

## REFERENCES

1. Bennet, F. F., and Yule, T. J., ANL-7763 (1971).
2. Ciallela, C. M., and Devanney, J. A., *Nucl. Instr. Meth.* 60:269 (1968).
3. Toms, M. E., *Nucl. Instr. Meth.* 92:61 (1971).
4. Johnson, R. H., and Wehring, B. W., ORNL/RSIC-40, p. 33 (1976).
5. Tsoulfanidis, N., Wehring, B. W., and Wyman, M. E., *Nucl. Instr. Meth.* 73:98 (1969).
6. Burrus, W. R., and Verbinski, V. V., *Nucl. Instr. Meth.* 67:181 (1969).
7. Kendrick, H., and Sperling, S. M., GA-9882 (1970).
8. Johnson, R. H., Ingersoll, D. T., Wehring, B. W., and Dorning, J. J., *Nucl. Instr. Meth.* 145:337 (1977).
9. Savitzky, A., and Golay, M. J. E., *Anal. Chem.* 36:1627 (1964).
10. Yule, H. P., *Nucl. Inst. Meth.* 54:61 (1967).
11. Yule, H. P., *Anal. Chem.* 38:103 (1966).
12. Johnson, R. H., Wehring, B. W., and Dorning, J. J., *Nucl. Sci. Eng.* 73:93 (1980).

MEASUREMENT AND DETECTION OF RADIATION
N. TSOULFANIDIS (McGRAW-HILL, 1983)

# 12

# gamma and x-ray spectroscopy

## 12.1 INTRODUCTION

Gamma and x-rays may be treated either as electromagnetic waves or as particles called photons. An *electromagnetic wave* is characterized by its wavelength $\lambda$ or frequency $\nu$. A *photon* is a particle having zero charge and zero rest mass, traveling with the speed of light, and having an energy $E = h\nu$, where $h$ = Planck's constant. The wave properties of a photon are used for low-energy measurements only. In all other cases, detection of photons is based on their interactions as particles.

This chapter first examines the mechanisms of detection in photon counters and then discusses the spectroscopic characteristics of the different types of x-ray and $\gamma$-ray detectors.

## 12.2 MODES OF ENERGY DEPOSITION IN THE DETECTOR

Photons are detected by means of the electrons they produce when they interact in the material of which the detector is made. The main interactions are photoelectric effect, Compton scattering, and pair production. The electrons (or positrons) produced by these interactions deposit their energy in the counter and thus generate a voltage pulse that signifies the passage of the photon. The height of the voltage pulse is proportional to the energy deposited in the detector. Since the objective is to measure the energy of the incident photon, the question arises: Is this voltage pulse proportional to the energy of the incident particle? To provide an answer, one must examine how the photon interacts and what happens to its energy.

### 12.2.1 Energy Deposition by Photons with $E < 1.022$ MeV

A photon with $E < 1.022$ MeV can interact only through the photoelectric or the Compton effect. If a photoelectric interaction takes place, the photon disappears and an electron appears with energy equal to $E - B$, where $B$ is the binding energy of that electron. The range of electrons in a solid, either a scintillator crystal or a semiconductor, is so short that it can be safely assumed that all the electron energy will be deposited in the detector (Fig. 12.1*a*). If the interaction occurs very close to the wall, the electron may deposit only part of its energy in the counter (Fig. 12.1*b*), but the probability of this happening is small. In practice, one assumes that all the photoelectrons deposit all their energy in the detector. This energy is less than the energy of the incident photon by the amount $B$, the binding energy of the electron. What happens to the energy $B$?

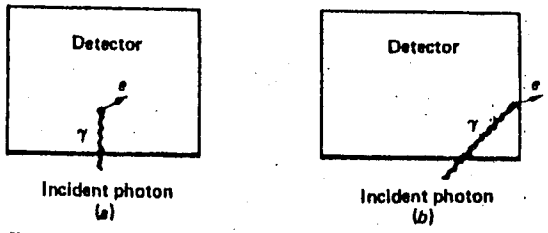


FIG. 12.1 As a result of a photoelectric interaction the photon disappears. In (*a*), all the energy of the electron is deposited in the detector. In (*b*), part of the energy is deposited in the wall.

After a photoelectric effect takes place, an electron from one of the outer atomic shells drops into the empty inner state in about $10^{-8}$ s. This electronic transition is followed by an x-ray or by an Auger electron (see Chap. 4). The Auger electron will also deposit its energy in the detector. The x-ray with energy in the low keV range (~ 100 keV or less) interacts again photoelectrically and generates another electron.† The net result of these successive interactions is that the part $B$ of the incident photon energy is also deposited in the counter. All these events take place within a time of the order of $10^{-8}$ s. Since the formation of the voltage pulse takes about $10^{-6}$ s, both parts of the energy—namely, $E - B$ = energy of photoelectron and $B$ = energy of the x-ray—contribute to the same pulse, the height of which is proportional to $(E - B) + B = E$ = incident photon energy. The conclusion is, therefore, that if the photon interacts via photoelectric effect, the resulting pulse has a height proportional to the incident particle energy.

If Compton scattering takes place, only a fraction of the photon energy is given to an electron. A scattered photon still exists carrying the rest of the energy. The energy of the electron is deposited in the detector. But what happens to the energy of the scattered photon?

The scattered photon may or may not interact again inside the detector. The probability of a second interaction depends on the size of the counter (Fig. 12.2), on

†For thin detectors, or detectors made of high-$Z$ material—e.g., CdTe or $HgI_2$—some x-rays may escape, thus forming the so-called "escape peaks" (see Sec. 12.9).

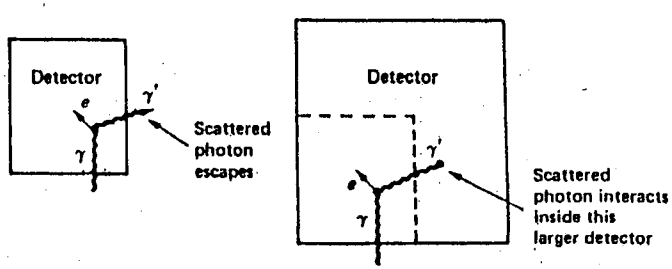


FIG. 12.2 As a result of Compton scattering, part of the photon energy may escape.



the position of the first interaction, on the energy of the scattered photon, and on the material of which the detector is made. Unless the detector is infinite in size, there is always a chance that the scattered photon may escape, in which case a pulse will be formed with height proportional to an energy which is *less* than the energy of the incident photon.

From the study of the Compton effect (Chap. 4), it is known that Compton electrons have an energy range from zero up to a maximum energy $T_{max}$ which is

$$T_{max} = E - \frac{E}{1 + 2E/mc^2} \tag{12.1}$$

where $mc^2 = 0.511$ MeV, the rest mass energy of the electron. Therefore, if the interaction is Compton scattering, pulses are produced from Compton electrons with heights distributed from $V = 0$ V, corresponding to $T_{min} = 0$, up to a maximum height $V_{max}$ corresponding to the maximum energy $T_{max}$. Figures 12.3 to 12.5 illustrate how a monoenergetic photon spectrum is recorded as a result of photoelectric and Compton interactions.

Figure 12.3 shows the source spectrum. In the case of perfect energy resolution, this monoenergetic source produces in an MCA the measured spectrum shown by Fig. 12.4. Some photons produce pulses that register in channel $C_0$, corresponding to the source energy $E_0$, and thus contribute to the main peak of the spectrum, which is called the full-energy peak. The Compton electrons are responsible for the continuous part of the spectrum, extending from zero channel up to channel $CC$ and called the *Compton continuum*. The end of the Compton continuum, called the *Compton edge*, corresponds to the energy given by Eq. 12.1. Since no detector exists with perfect energy resolution, the measured spectrum looks like that of Fig. 12.5.

Sometimes the Compton interaction occurs very close to the surface of the detector or in the material of the protective cover surrounding the detector (Fig. 12.6).† Then there is a high probability that the electron escapes and only the energy of the scattered photon is deposited in the detector. The minimum energy $E_{min}$ of the scattered photon is given by

$$E_{min} = \frac{E}{1 + 2E/mc^2} \tag{12.2}$$

†Backscattering may also take place in the source itself, or in the shield surrounding the detector.

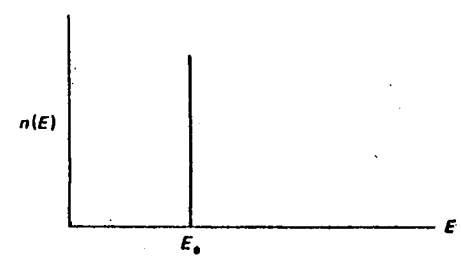


FIG. 12.3 A monoenergetic gamma spectrum (source spectrum).

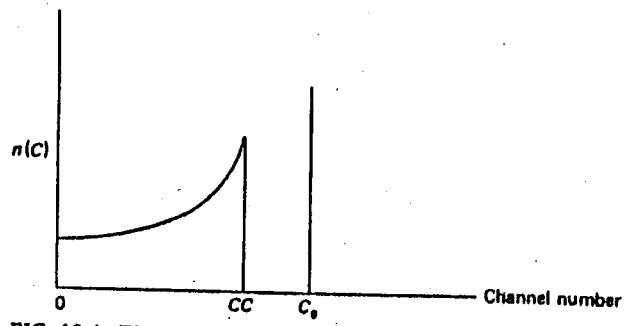


FIG. 12.4 The pulse height spectrum obtained from the source spectrum of Fig. 12.3, in the absence of statistical effects in the detector (perfect energy resolution).

Occasionally a rather broad peak, corresponding to the energy given by Eq. 12.2, is observed in $\gamma$-ray spectra. This peak is called the *backscatter peak* (Fig. 12.5).

The fraction of counts recorded outside the full-energy peak depends on the energy of the gamma and on the size of the detector. The energy of the photon determines the ratio $\sigma/\mu$ of the Compton scattering coefficient to the total attenuation coefficient. The lower the gamma energy is, the smaller this ratio becomes. Then a greater fraction of particles interacts photoelectrically and is recorded in the full-energy peak, thus reducing the Compton continuum part of the spectrum. As an example, consider gammas with energy 100 keV and 1 MeV, and a Ge(Li) detector. For 100-keV gammas in germanium, the ratio $\sigma/\mu$ is $0.9/3.6 \approx 0.25$ (Fig. 12.27), which indicates that 25 percent of the interactions are Compton and 75 percent photoelectric. The number of pulses in the Compton continuum should be equal to or less than one-third the number recorded under the full-energy peak. At 1 MeV, the

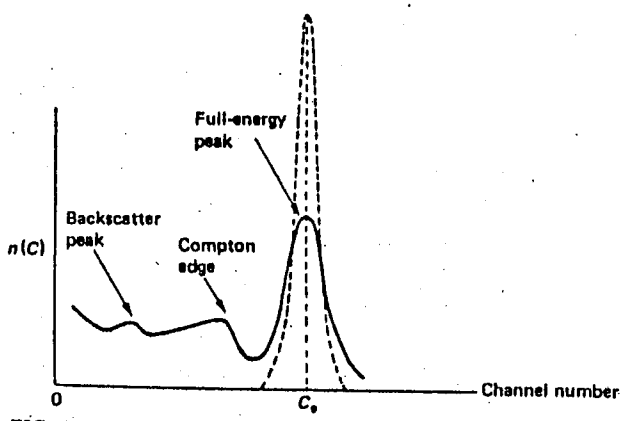


FIG. 12.5 The measured pulse height spectrum for the source spectrum of Fig. 12.3. The statistical effects in the detector broaden both the peak and the Compton continuum part of the spectrum. The dashed line shows the spectrum that would have been recorded in the absence of the Compton continuum.



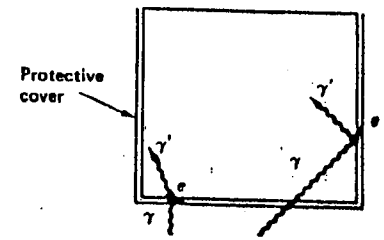


FIG. 12.6 If Compton scattering occurs close to the surface of the detector, the only energy deposited may be that of the scattered photon.

ratio $\sigma/\mu$ is about $0.4/0.42 \approx 0.95$, which means that about 95 percent of the interactions are Compton and only 5 percent photoelectric. Thus, the Compton continuum due to 1-MeV photons is the largest part of the spectrum.

The magnitude of the Compton continuum is also affected by the size of the detector (Fig. 12.2). The larger the detector is, the greater the probability of a second Compton interaction. If the detector size could become infinite, the Compton continuum would disappear.

### 12.2.2 Energy Deposition by Photons with $E > 1.022$ MeV

If $E > 1.022$ MeV, pair production is possible, in addition to photoelectric effect and Compton scattering. As a result of pair production, the photon disappears and an electron-positron pair appears, at the expense of 1.022 MeV transformed into the pair's rest masses. The total kinetic energy of the electron-positron pair is

$$T_{e^-} + T_{e^+} = T = E - 1.022 \text{ MeV}$$

The kinetic energy of the pair is deposited in the counter (the arguments are the same as for photoelectrons or Compton electrons). Therefore, pulses proportional to the energy $T = E - 1.022$ MeV are certainly produced. But, what happens to the energy of 1.022 MeV?

The positron slows down and reaches the end of its range in a very short time, shorter than the time needed for pulse formation. Sometimes while in flight, but most of the time at the end of its track, it combines with an atomic electron, the two annihilate, and two gammas are emitted, each with energy 0.511 MeV.† There are several possibilities for the fate of these annihilation gammas.

1 The energy of both annihilation gammas is deposited in the detector. Then, a pulse height proportional to energy

$$(E - 1.022) + 1.022 = E$$

is produced.

†There is a small probability that three gammas may be emitted. This event has a negligible effect on spectroscopy measurements.

2 Both annihilation photons escape. A pulse height proportional to energy $E - 1.022$ MeV is formed.
3 One annihilation photon escapes. A pulse height proportional to energy

$$E - 1.022 \text{ MeV} + 0.511 \text{ MeV} = E - 0.511 \text{ MeV}$$

is formed.

If the pair production event takes place on or close to the surface of the detector, it is possible that only one of the annihilation photons enters the counter. In such a case, a pulse height proportional to energy 0.511 MeV is formed.

Peaks corresponding to these energies could be identified, but this does not mean that they are observed in every $\gamma$-ray spectrum. The number, energy, and intensity of peaks depends on the size of the detector, the geometry of the source (is it collimated or not?), and the energies of the gammas in the spectrum. If a source emits only one gamma, the measured spectrum will certainly show:

1 The full-energy peak, corresponding to $E$ (this is the highest energy peak)
2 The Compton edge, corresponding to energy

$$E - \frac{E}{1 + 2E/mc^2}$$

Other peaks that may be observed are:

3 Backscatter peak, with energy

$$\frac{E}{1 + 2E/mc^2}$$

4 The *single-escape peak* with energy $(E - 0.511)$ MeV
5 The *double-escape peak* with energy $(E - 1.022)$ MeV

Figure 12.7 presents the spectrum of $^{24}$Na. The single- and double-escape peaks due to the 2.754-MeV gamma are clearly shown. The single- and double-escape peaks are very important when complex gamma spectra are recorded. The observer should be extremely careful to avoid identifying them falsely as peaks produced by gammas emitted from the source.

If the source is a positron emitter, a peak at 0.511 MeV is always present. The positron-emitting isotope $^{22}$Na is such an example. It emits only one gamma with energy 1.274 MeV, yet its spectrum shows two peaks. The second peak is produced by 0.511-MeV annihilation photons emitted after a positron annihilates (Fig. 12.8).

The Compton continuum, present in gamma energy spectra recorded either by a NaI(Tl) scintillator or by a Ge(Li) detector, is a nuisance that impedes the analysis of complex spectra. It is therefore desirable to eliminate or at least reduce that part of the spectrum relative to the gamma-energy peak. One way to achieve this is to use two detectors and operate them in anticoincidence. Such an arrangement, known as the *Compton-suppression spectrometer*, is shown in Fig. 12.9. A large NaI(Tl) scintil-



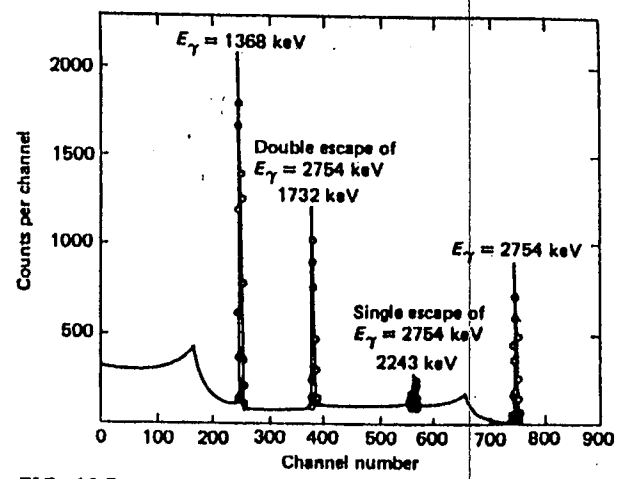


FIG. 12.7 A gamma spectrum showing single- and double-escape peaks (from Chap. 4.4.2 of Bertolini-Coche).

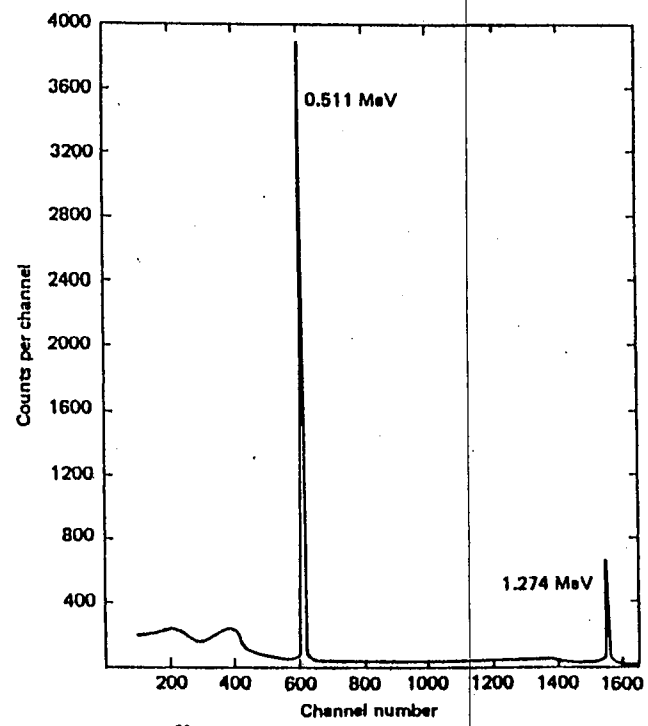


FIG. 12.8 The $^{22}$Na spectrum showing the 1.274-MeV peak and the 0.511-MeV peak that is due to annihilation gammas.

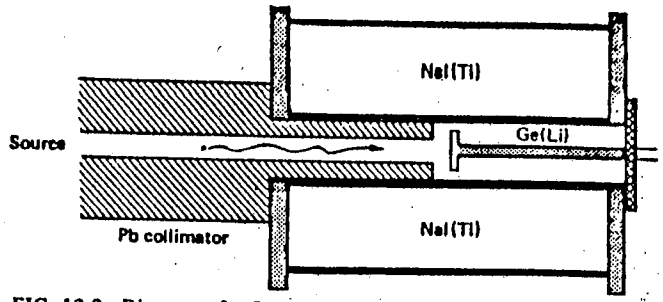


FIG. 12.9 Diagram of a Compton suppression spectrometer using a NaI(Tl) and a Ge(Li) detector. The two detectors are operated in anticoincidence, with the Ge(Li) recording the energy spectrum.

lator surrounds a Ge(Li) detector, and the two detectors are operated in anticoincidence. The energy spectrum of the central detector [the Ge(Li) in this case] will consist of pulses that result from total energy absorption in that detector. Figure 12.10 shows the $^{60}$Co spectrum obtained with and without Compton suppression.

## 12.3 EFFICIENCY OF X-RAY AND GAMMA-RAY DETECTORS: DEFINITIONS

There are four types of efficiency reported in the literature:

1 Total detector efficiency
2 Full-energy peak efficiency
3 Double-escape peak efficiency
4 Single-escape peak efficiency

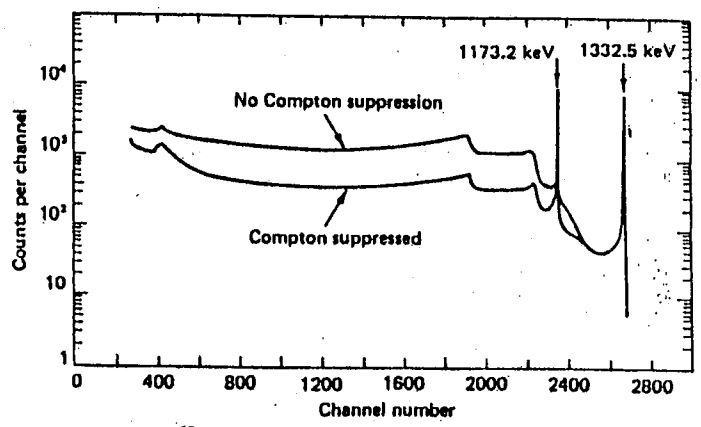


FIG. 12.10 The $^{60}$Co spectrum recorded with and without Compton suppression. Notice that the ordinate is in logarithmic scale.



The first two are much more frequently used than the last two. All four efficiencies may be intrinsic, absolute, or relative. The individual definitions are as follows.

*Intrinsic total detector efficiency* is the probability that a gamma of a given energy which strikes the detector will be recorded. The geometry assumed for the calculation or measurement of this efficiency is shown in Fig. 12.11.

*Absolute total detector efficiency* is the probability that a gamma emitted from a specific source will be recorded in the detector. The geometry assumed for the absolute efficiency is shown in Fig. 12.12. The intrinsic efficiency (Fig. 12.11) depends on the energy of the gamma, $E$, and the size of the detector $L$. The total efficiency (Fig. 12.12) depends on, in addition to $E$ and $L$, the radius of the detector $R$ and the source-detector distance $d$. Therefore the total efficiency, as defined here, is the product of intrinsic efficiency times the solid angle fraction (see also Chap. 8).

*Full-energy peak efficiency* is defined as follows:

$$\begin{pmatrix}\text{Full-energy peak}\\ \text{efficiency}\end{pmatrix} = \begin{pmatrix}\text{total detector}\\ \text{efficiency}\end{pmatrix} \times \frac{\begin{pmatrix}\text{counts in full-}\\ \text{energy peak}\end{pmatrix}}{\begin{pmatrix}\text{total counts in}\\ \text{spectrum}\end{pmatrix}} \tag{12.3}$$

The ratio by which the total detector efficiency is multiplied in Eq. 12.3 is called the *peak-to-total ratio* ($P$). Figure 12.13 shows how $P$ is measured.

The *double-escape peak efficiency* is important if the energy of the gamma $E$ is greater than about 1.5 MeV, in which case pair production becomes important. The energy of the double-escape peak, equal to $E - 1.022$ MeV, is used for identification of certain isotopes. This kind of efficiency is defined by

$$\begin{pmatrix}\text{Double-escape}\\ \text{peak efficiency}\end{pmatrix} = \begin{pmatrix}\text{total detector}\\ \text{efficiency}\end{pmatrix} \times \frac{\begin{pmatrix}\text{counts in double-}\\ \text{escape peak}\end{pmatrix}}{\begin{pmatrix}\text{total counts in}\\ \text{spectrum}\end{pmatrix}} \tag{12.4}$$

The *single-escape peak efficiency* is important also for $E > 1.5$ MeV, and its definition is analogous to that of the double-escape peak.

$$\begin{pmatrix}\text{Single-escape}\\ \text{peak efficiency}\end{pmatrix} = \begin{pmatrix}\text{total detector}\\ \text{efficiency}\end{pmatrix} \times \frac{\begin{pmatrix}\text{counts in single-}\\ \text{escape peak}\end{pmatrix}}{\begin{pmatrix}\text{total counts in}\\ \text{spectrum}\end{pmatrix}} \tag{12.5}$$

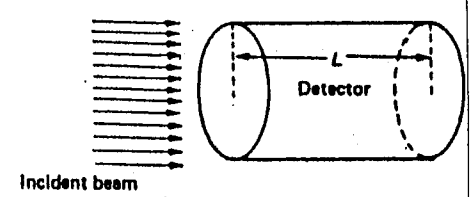


FIG. 12.11 The geometry assumed in the definition of intrinsic efficiency.

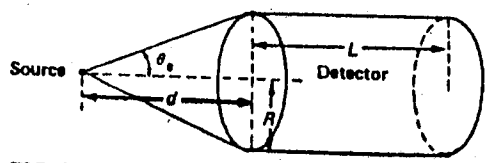


FIG. 12.12 The geometry assumed in the definition of absolute efficiency.

The double- and single-escape peak efficiencies are used with semiconductor detectors only. In the above definitions, if the total detector efficiency is replaced by intrinsic, the corresponding full-energy, single-, and double-escape peak efficiencies are also considered intrinsic.

*Relative* efficiency may be obtained for all the cases discussed above. In general,

$$(\text{Relative efficiency})_i = \frac{(\text{absolute efficiency})_i}{\text{efficiency of a standard}} \tag{12.6}$$

where the subscript $i$ refers to any one of the efficiencies defined earlier.

## 12.4 DETECTION OF PHOTONS WITH NaI(Tl) SCINTILLATION COUNTERS

Of all the scintillators existing in the market, the NaI crystal activated with thallium, NaI(Tl), is the most widely used for the detection of $\gamma$ rays. NaI(Tl) scintillation

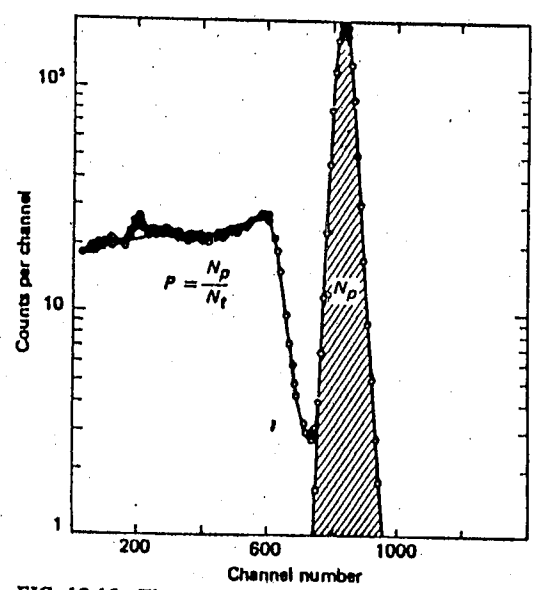


FIG. 12.13 The peak-to-total ratio is equal to the number of counts under the peak ($N_p$) divided by the total number of counts ($N_t$).



counters are used when the energy resolution is not the most important factor of the measurement. They have the following advantages over Ge(Li) and Si(Li) detectors:

1 They can be obtained in almost any shape and size. NaI(Tl) crystals with size 0.20 m (8 in) diameter by 0.20 m (8 in) thickness are commercially available.
2 They have rather high efficiency (see Sec. 12.3.1).
3 They cost less than semiconductor detectors.

A disadvantage of all scintillation counters, in addition to their inferior energy resolution relative to Si(Li) and Ge(Li) detectors, is the necessary coupling to a photomultiplier tube.

NaI(Tl) detectors are offered in the market today either as crystals that may be ordered to size or as integral assemblies mounted to an appropriate photomultiplier tube.[1-3] The integral assemblies are hermetically sealed by an aluminum housing. Often, the housing is chrome-plated for easier cleaning. The phototube itself is covered by an antimagnetic $\mu$-metal that reduces gain perturbations caused by electric and magnetic fields surrounding the unit.

The front face of the assembly is usually the "window" through which the photons pass before they enter into the crystal. The window should be as thin as possible to minimize the number of interactions of the incident photons in the materials of the window. Commercially available NaI(Tl) counters used for $\gamma$-ray detection have an aluminum window, which may be as thin as 0.5 mm (0.02 in). X-ray scintillation counters usually have a beryllium window, which may be as thin as 0.13 mm (0.005 in). Beryllium is an excellent material because it causes less absorption thanks to its low atomic number ($Z = 4$).

### 12.4.1 Efficiency of NaI(Tl) Detectors

The intrinsic efficiency of NaI(Tl) detectors (see Fig. 12.11) is essentially equal to $1 - \exp[-\mu(E)L]$, where

$\mu(E)$ = total attenuation coefficient in NaI for photons with energy $E$

$L$ = length of the crystal

A plot of $\mu(E)$ for NaI as a function of photon energy is shown in Fig. 12.14.

The efficiency increases with crystal size. The user should be aware, however, that when the detector volume increases, the background counting rate increases too. In fact, the background is roughly proportional to the crystal volume, while the efficiency increases with size at a slower than linear rate. Thus, there may be a practical upper limit to a useful detector size for a given experiment.

Calculated total efficiencies of a NaI crystal are given in Fig. 12.15 for several source-detector distances. They have been obtained by integrating Eq. 8.20, which is repeated here (refer to Fig. 12.12 for symbols):

$$\epsilon(E) = \frac{\int_0^{\theta_0} S\{1 - \exp[-\mu(E)r(\theta)]\}\frac{1}{2}\sin\theta\, d\theta}{(S/2)\int_0^{\theta_0} \sin\theta\, d\theta} \tag{8.20}$$

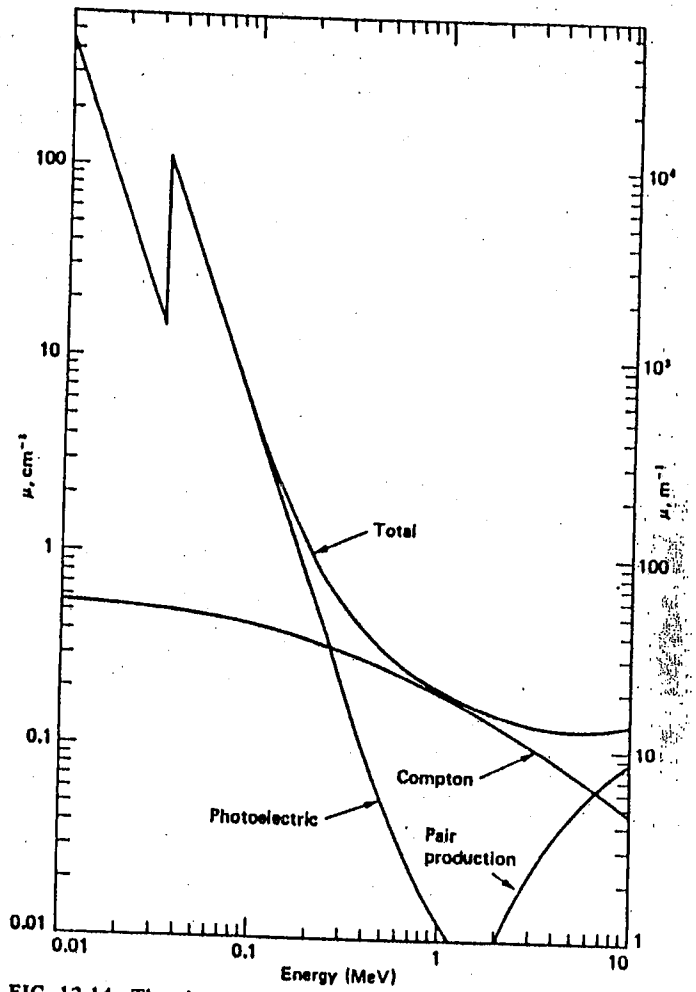


FIG. 12.14 The photon attenuation coefficients for NaI(Tl) (from ref. 3).

or,

$$\epsilon(E) = \frac{\int_0^{\theta_1} \{1 - \exp[-\mu(E)L/\cos\theta]\} \sin\theta \, d\theta}{1 - \cos\theta_0} + \frac{\int_{\theta_1}^{\theta_0} (1 - \exp\{-\mu(E)[(L/\sin\theta) - (d/\cos\theta)]\}) \sin\theta \, d\theta}{1 - \cos\theta_0}$$

where $\theta_1 = \tan^{-1}(R/d + L)$
$\theta_0 = \tan^{-1}(R/d)$



In Fig. 12.15, note that the efficiency decreases with energy up to about 5 MeV. Beyond that point, it starts increasing because of the increase in the pair production probability. Figure 12.16 shows how the peak-to-total ratio (see Fig. 12.13) changes with energy for a source located 0.10 m from detectors of different sizes.

### 12.4.2 Analysis of Scintillation Detector Energy Spectra

NaI(Tl) scintillators are seldom used as gamma-ray spectrometers because their energy resolution is inferior to that of semiconductor detectors. Despite this fact, a brief discussion of the methods of analysis of NaI(Tl) spectra is instructive because it helps point out differences and similarities between the responses of NaI(Tl) and Ge(Li) detectors.

If a NaI(Tl) scintillator is used to detect a photon spectrum consisting of many gamma energies, the measured spectrum will be the summation of spectra similar to those shown in Fig. 12.5. To identify individual energies from a complex spectrum, one unfolds the measured spectrum (see Chap. 11). Unfolding, in turn, requires the knowledge of the detector response function.

Response functions of NaI(Tl) detectors, obtained by Heath et al.,[4,5] are shown in Fig. 12.17. These authors measured the response for several gamma energies and then used an interpolation scheme to derive the three-dimensional plot of Fig. 12.17. A modified Gaussian of the form

$$y(x) = y_0 \left\{ 1 + \alpha_1 (x - x_0)^4 + \alpha_2 (x - x_0)^{12} \exp\left[ -\frac{(x - x_0)^2}{b_0} \right] \right\} \tag{12.7}$$

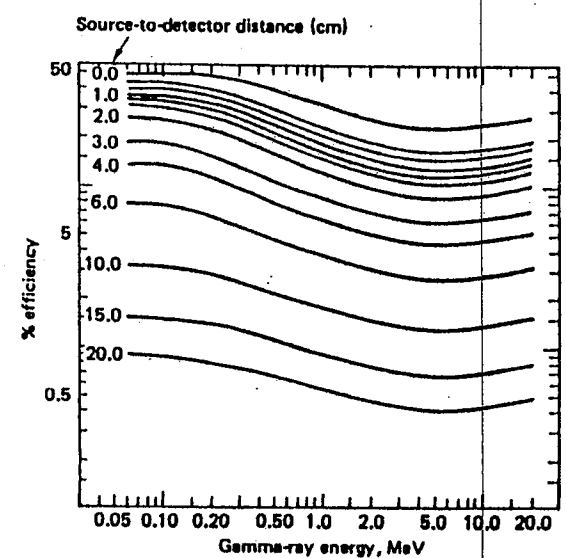


FIG. 12.15 Calculated efficiencies of a 3" X 3" (76.2-mm X 76.2-mm) NaI(Tl) scintillator as a function of energy for different source-detector distances (from ref. 3).

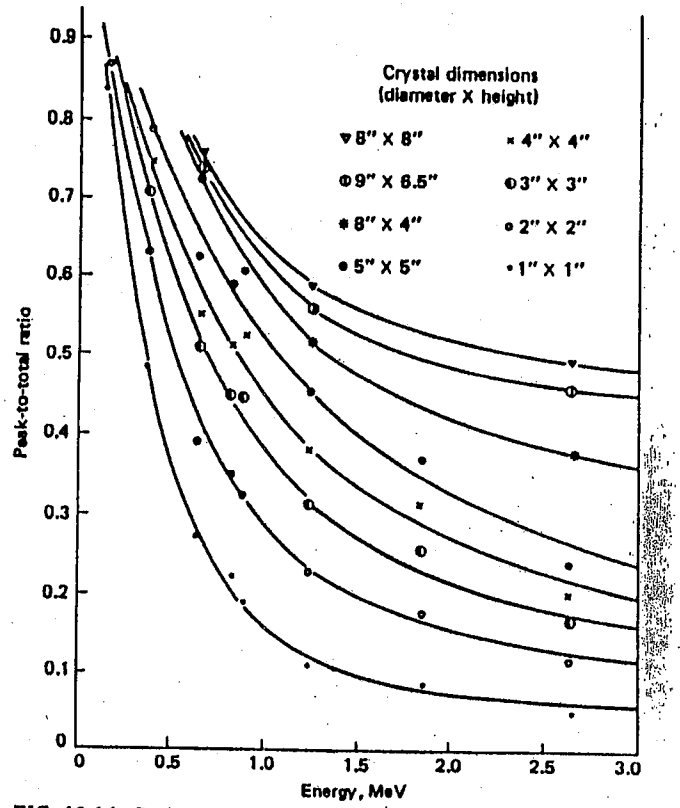


FIG. 12.16 Peak-to-total ratio as a function of energy for NaI(Tl) scintillators of different sizes. The source-to-detector distance is 0.10 m (from ref. 3).

gave a successful fit to individual gamma peaks. The five parameters $y_0$, $x_0$, $b_0$, $\alpha_1$, and $\alpha_2$ were determined by least-squares fit. The parameter $x_0$ shows the location of the peak, and $b_0$ is related to the FWHM by $\Gamma = 2\sqrt{2(\ln 2)b_0}$. Figure 12.18 shows the measured and calculated response functions for $^{137}$Cs. Unfolding of the spectrum was achieved by using these response functions in a computer program that determines energy and intensity of individual gammas based on a least-squares and iteration technique.[5]

The energy resolution of NaI(Tl) detectors is quoted in terms of the percent resolution for the 0.662-MeV gamma of $^{137}$Cs. At the present time (1982), using the best electronics available, this resolution is about 6 percent and the FWHM is about 40 keV. As mentioned in Chap. 9, the FWHM is roughly proportional to the square root of the energy. For this reason, the resolution in percent deteriorates as the energy decreases. For 10-keV x-rays, the best resolution achieved is about 40 percent, which makes the FWHM about 4 keV.



## 12.5 DETECTION OF GAMMAS WITH AN NE 213 ORGANIC SCINTILLATOR

The NE 213 organic scintillator has emerged as one of the leading fast neutron spectrometers (see Chap. 14). As a gamma spectrometer, the NE 213 scintillator has an efficiency lower than that of NaI(Tl) and an energy resolution which is poor compared to that of semiconductor detectors. There are certain applications, however, where high energy resolution is not the most important factor. One such application is detection of gammas in a mixed neutron-gamma field. There, the ability of the NE 213 scintillator to discriminate against neutrons makes it an attractive gamma detector.

Because gammas are detected by the NE 213 scintillator mainly through Compton interactions, the response function of the detector consists of the Compton continuum. The response function has been calculated[6] and measured[7] for several gamma

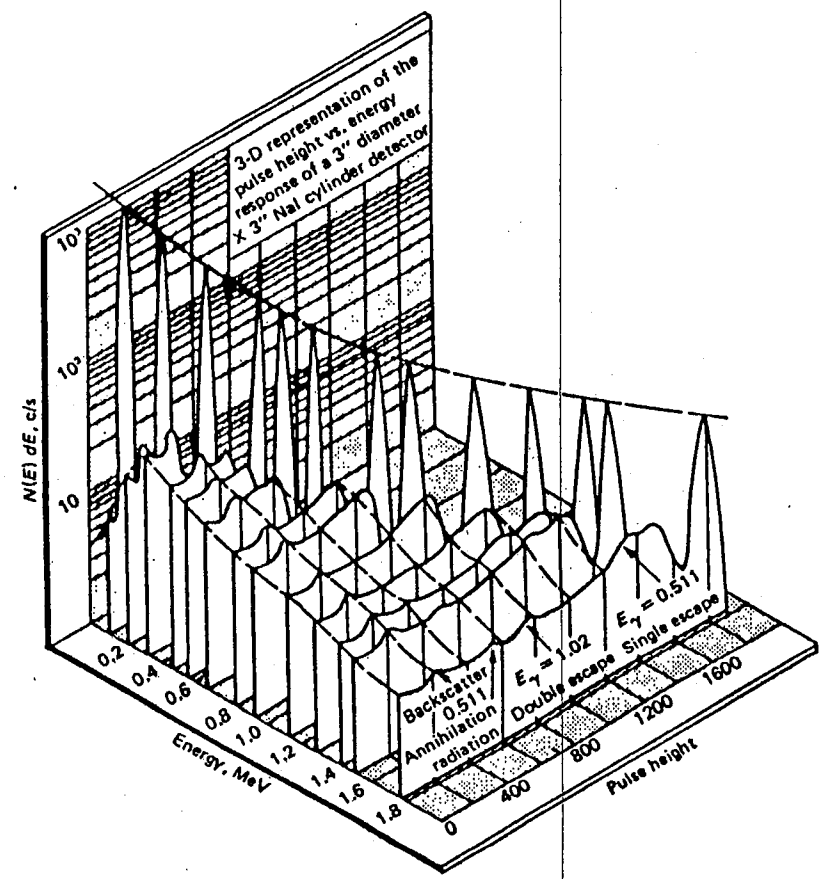


FIG. 12.17 A three-dimensional representation of NaI(Tl) response functions (from ref. 4).

## 4.8 COMMAND KEY SUMMARY

A condensed listing of **standard key commands** follows:

| | |
|---|---|
| F1 | Toggle data acquisition. |
| F2 | Toggle erase enable. |
| Ctrl F2 | Erase spectrum if erase enabled. |
| F3 | Preset data acquisition time. |
| Alt X | Exit to DOS |
| Up-Arrow | Increase the vertical scale. Increase display offset |
| Down-Arrow | Decrease the vertical scale. Decrease display offset |
| Right-Arrow | Move the cursor one channel to the right. |
| Left-Arrow | Move the cursor one channel to the left. |
| Page-Up | Move the cursor right 1/32 of the display. |
| Page-Down | Move the cursor left 1/32 of the display. |
| Ctrl-Home | Move the cursor to channel zero. |
| Ctrl-End | Move the cursor to the last channel. |
| Ctrl Left Arrow | Move cursor one pixel column to the right. |
| Ctrl Right Arrow | Move cursor one pixel column to the left. |
| Ctrl Page Up | Move cursor one ROI to the right. |
| Ctrl Page Down | Move cursor one ROI to the left. |
| Home | Move the cursor to first channel in window. |
| End | Move the cursor to last channel in window. |
| Alt A | Toggle centroid and resolution calculations. |
| Alt R | Toggle ROI display mode. |
| Esc | Toggle between menu key bars. Aborts long calculations. |
| F4 | Select expanded display mode. |
| F5 | Enter a spectrum identification code. |
| F6 | Load a binary spectrum file into memory. |
| F7 | Save a spectrum as a binary disk file. |
| Del | Clear ROI containing current cursor channel. |
| F9 | Start ROI in current channel. |
| Alt F9 | Select ROI display colors. |
| F10 | End ROI in current channel. |

**Pull-Down Menu Keys**

| | |
|---|---|
| Right Arrow | Move one menu to the right. |
| Left Arrow | Move one menu to the left. |
| Up Arrow | Move up one menu choice. |
| Down Arrow | Move down one menu choice. |
| Page Up | Move to first menu choice. |
| Page Down | Move to last menu choice. |
| Home | Move to first menu choice. |
| End | Move to last menu choice. |
| Esc | Exit pull-down menu. |
| Return | Select current menu choice. |

**Line Editor Keys**

| | |
|---|---|
| Right Arrow | Move the cursor one character to the right. |
| Left Arrow | Move the cursor one character to the left. |
| Home | Move to first character position. |
| End | Move to end of edit data. |
| Insert | Toggle between insert and overlay modes. |
| Ctrl Y | Delete entire line of data. |
| Back Arrow | Destructive backspace. |
| Del | Delete current character. |
| Esc | Exit editor void current work. |
| Return | Exit editor accept current work. |

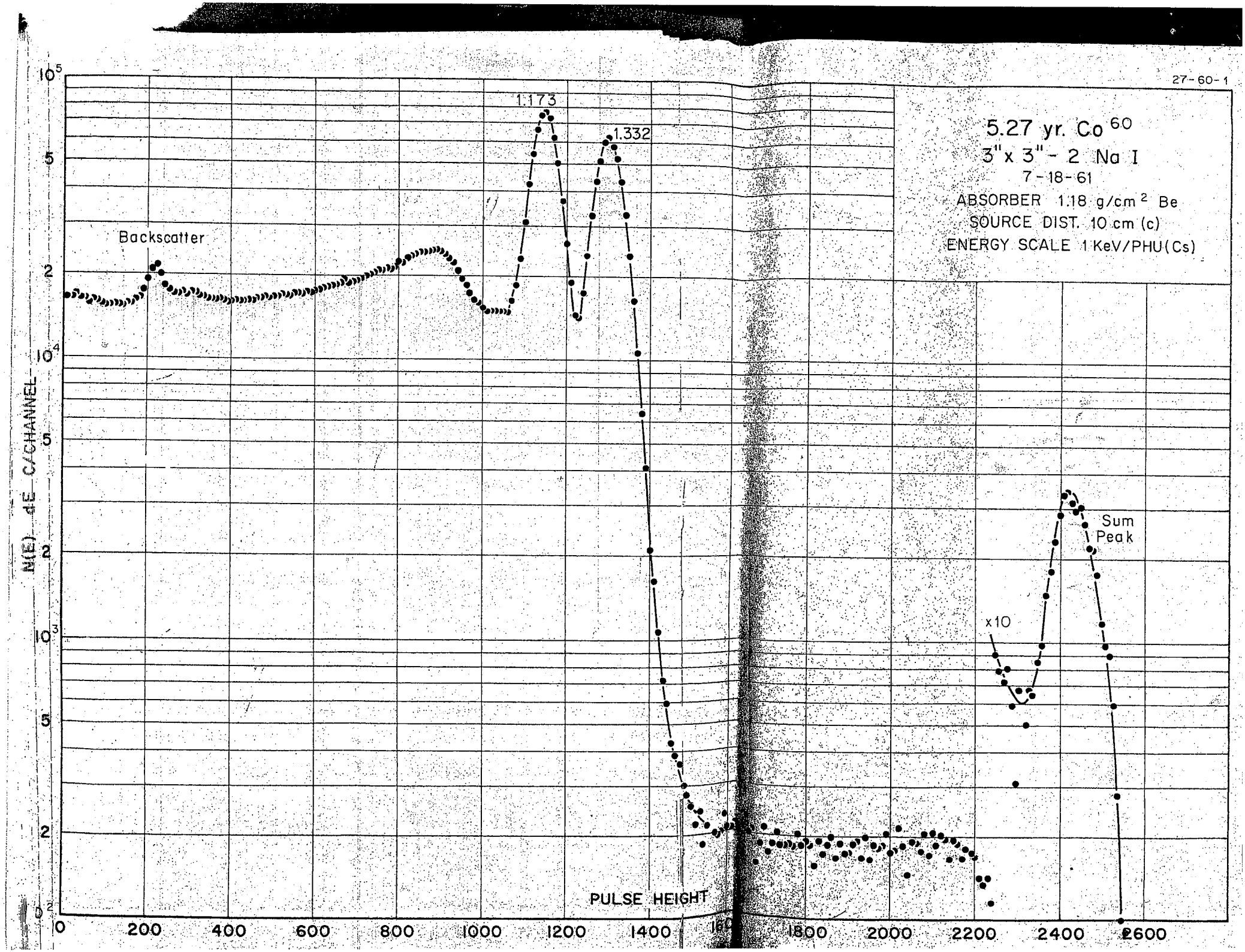
27-60-1
5.27 yr. Co 60
3" x 3" - 2 Na I
7-18-61
ABSORBER 1.18 g/cm 2 Be
SOURCE DIST. 10 cm (c)
ENERGY SCALE 1 KeV/PHU(Cs)
1.173
1.332
Backscatter
Sum Peak
x10
N(E) dE C/CHANNEL
PULSE HEIGHT
10 5
5
2
10 4
5
2
10 3
5
2
10 2
0
200
400
600
800
1000
1200
1400
1600
1800
2000
2200
2400
2600

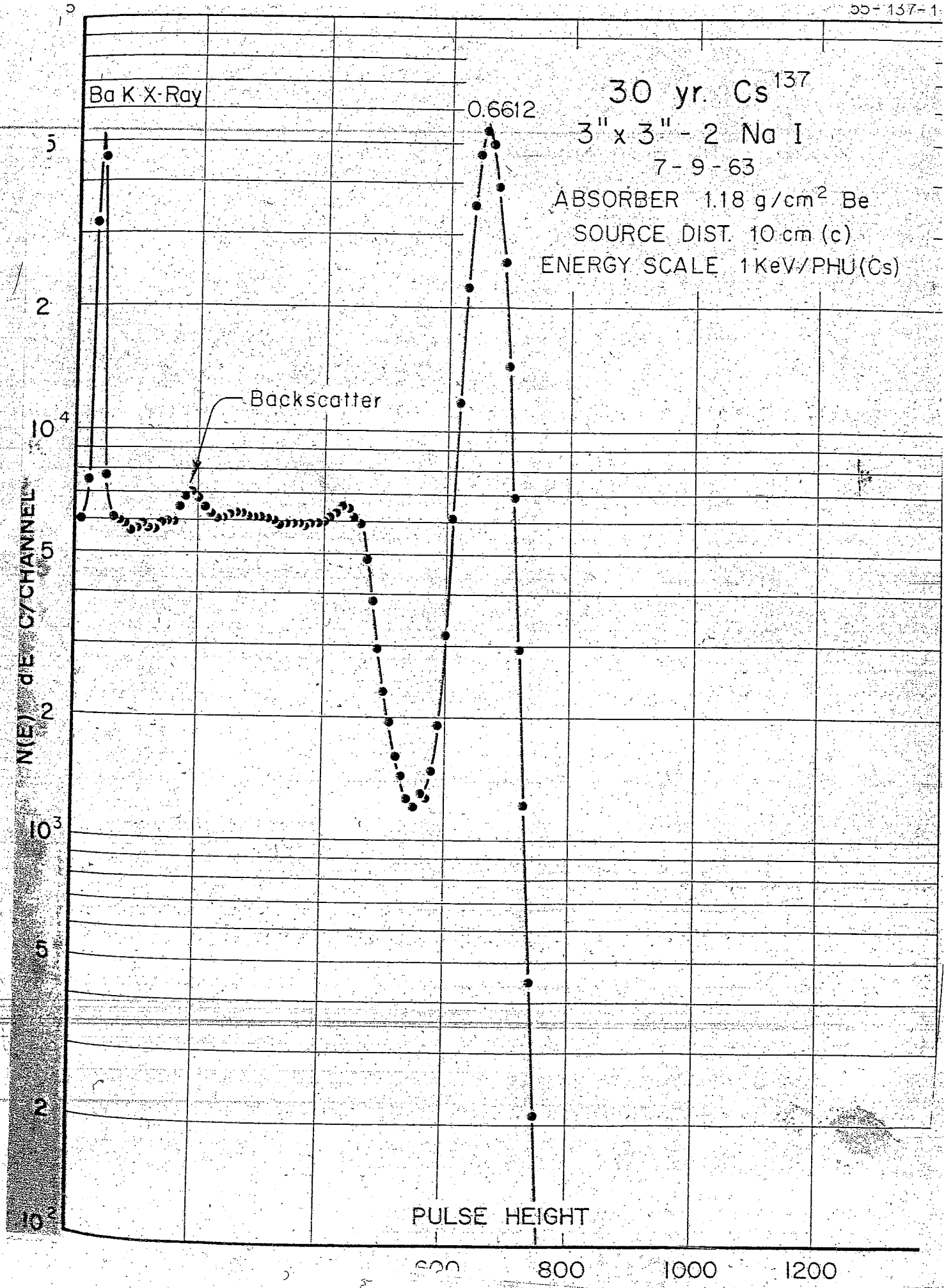
30 yr. Cs137
3" x 3" - 2 Na I
7-9-63
ABSORBER 1.18 g/cm2 Be
SOURCE DIST. 10 cm (c)
ENERGY SCALE 1 KeV/PHU(Cs)
Ba K X-Ray
0.6612
Backscatter
N(E) dE C/CHANNEL
PULSE HEIGHT
600
800
1000
1200

[redacted] ACTIVATION [redacted]

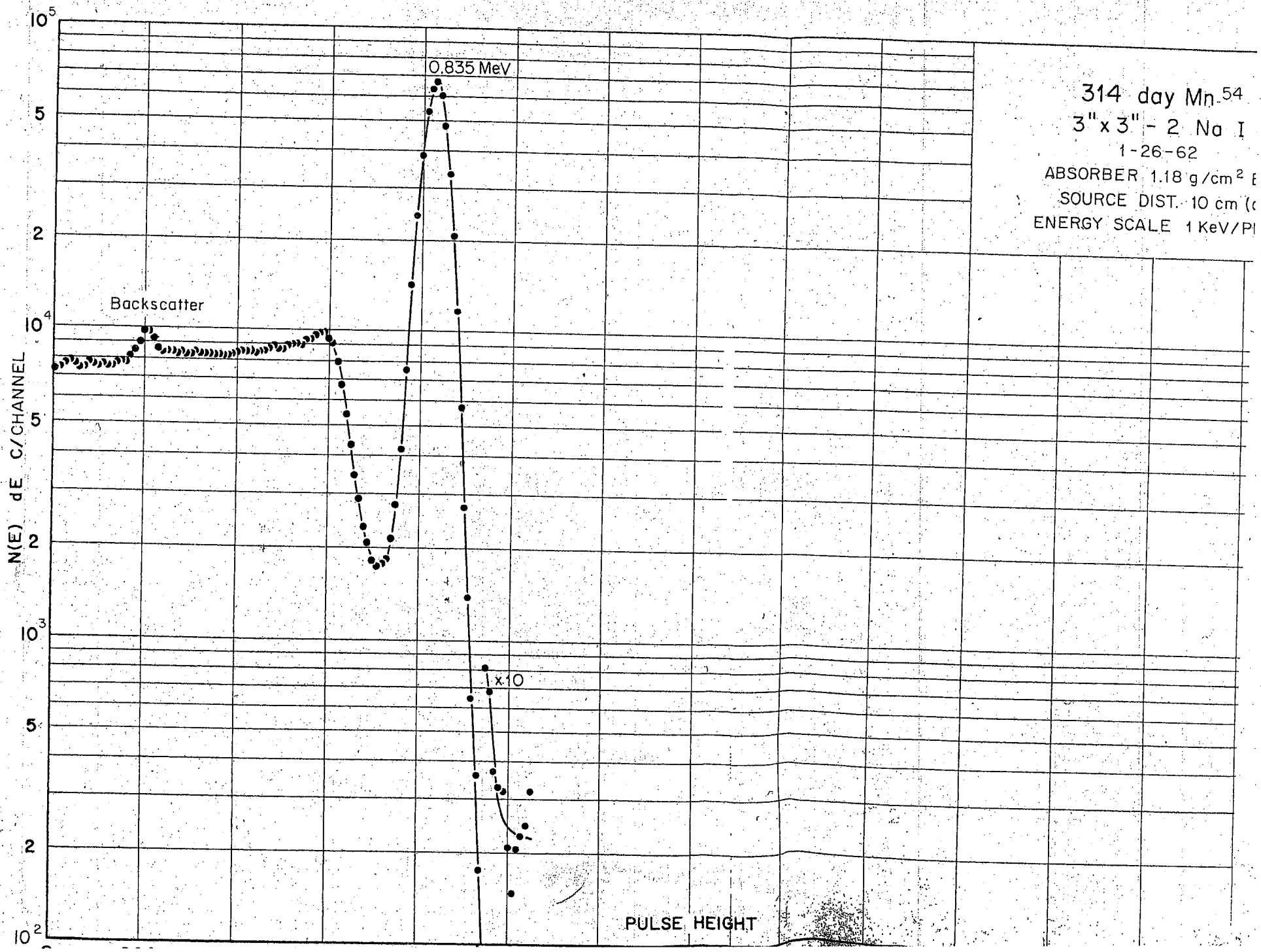

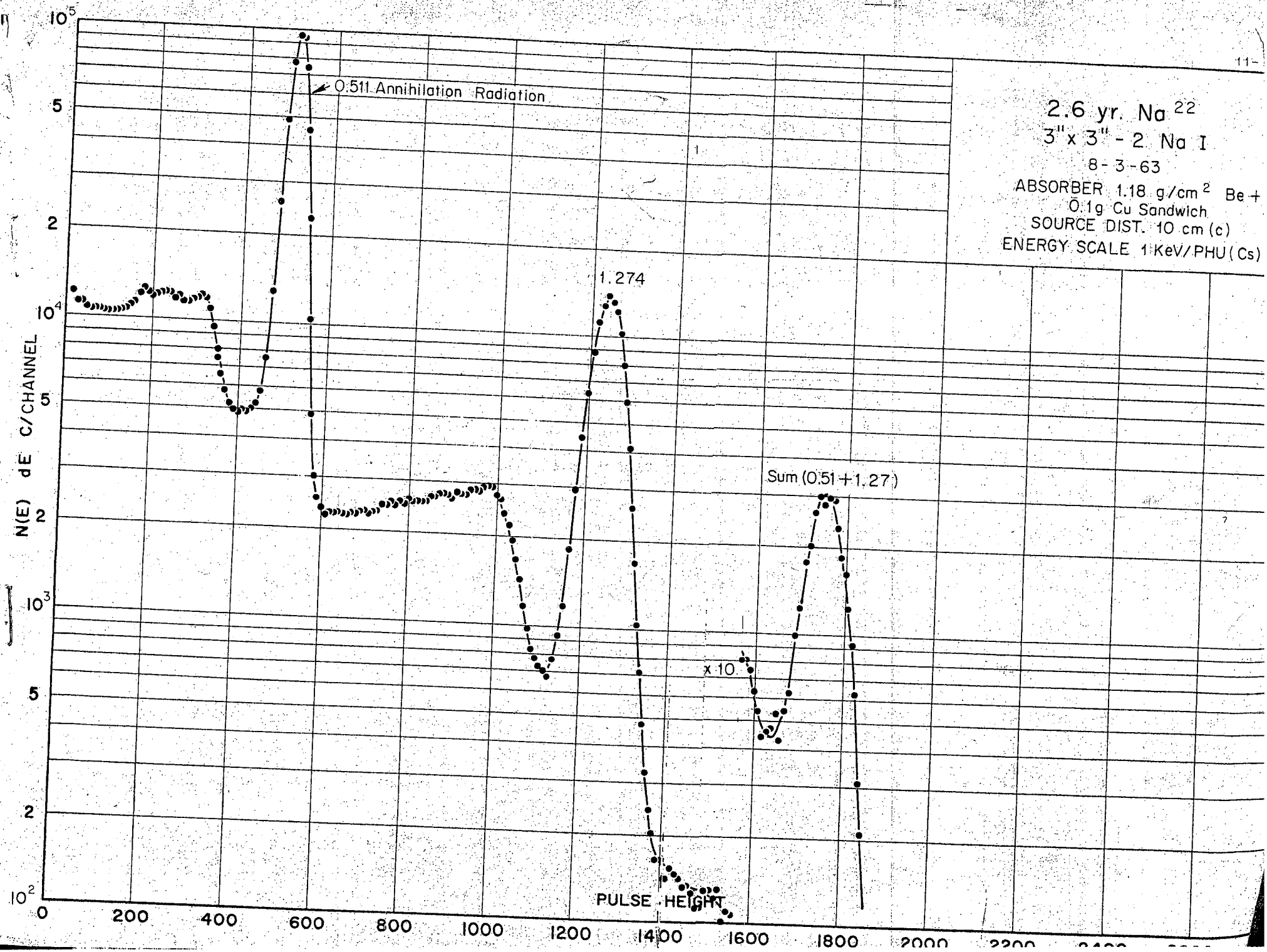
11-
2.6 yr. Na 22
3" x 3" - 2 Na I
8-3-63
ABSORBER 1.18 g/cm 2 Be +
0.1g Cu Sandwich
SOURCE DIST. 10 cm (c)
ENERGY SCALE 1 KeV/PHU (Cs)
0.511 Annihilation Radiation
1.274
Sum (0.51 + 1.27)
x 10
N(E) dE C/CHANNEL
PULSE HEIGHT
10^5
5
2
10^4
5
2
10^3
5
2
10^2
0
200
400
600
800
1000
1200
1400
1600
1800
2000
2200

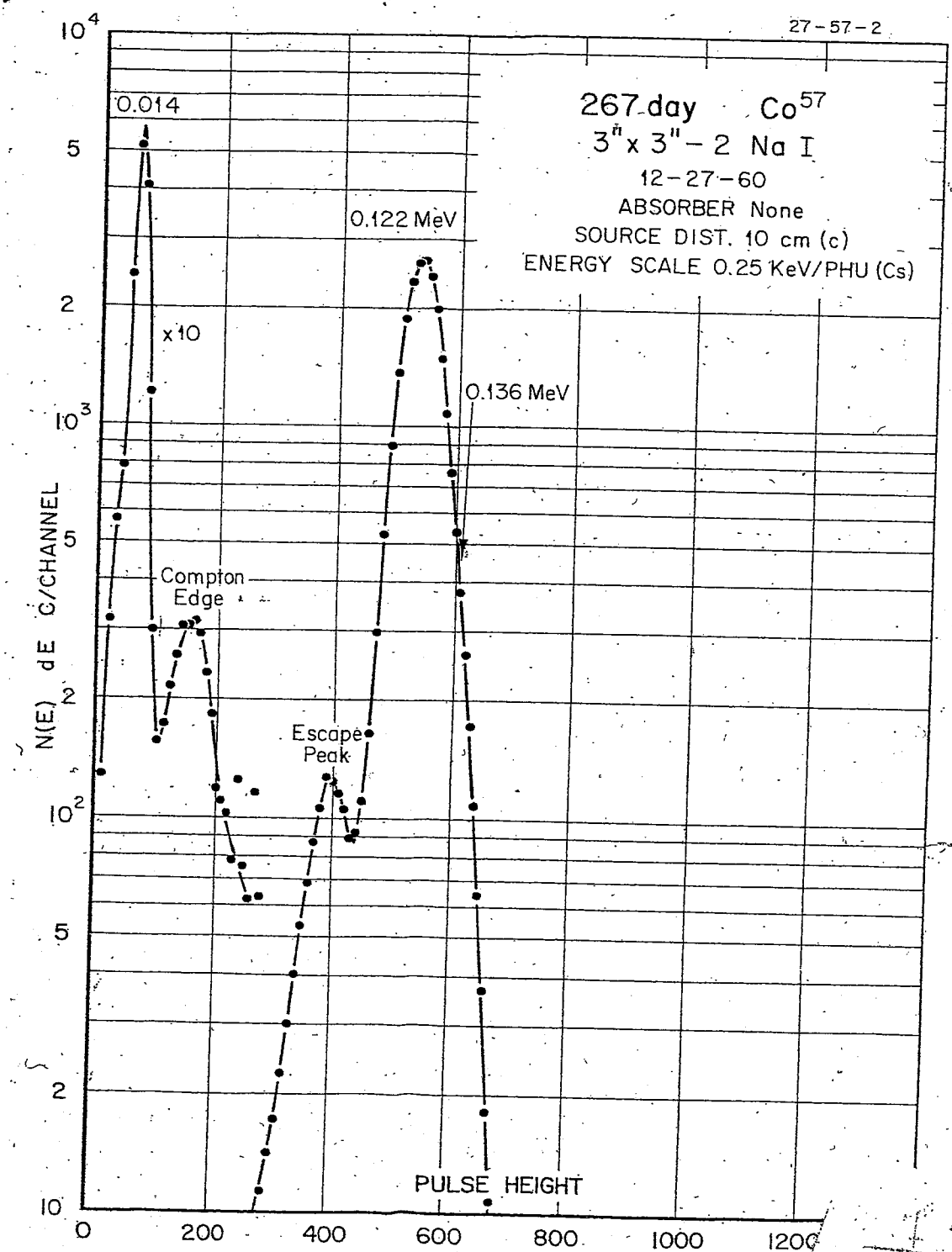
27-57-2
267 day Co57
3" x 3" - 2 Na I
12-27-60
ABSORBER None
SOURCE DIST. 10 cm (c)
ENERGY SCALE 0.25 KeV/PHU (Cs)
0.014
x10
0.122 MeV
0.136 MeV
Compton Edge
Escape Peak
N(E) dE C/CHANNEL
PULSE HEIGHT
10^4
5
2
10^3
5
2
10^2
5
2
10
0
200
400
600
800
1000
1200

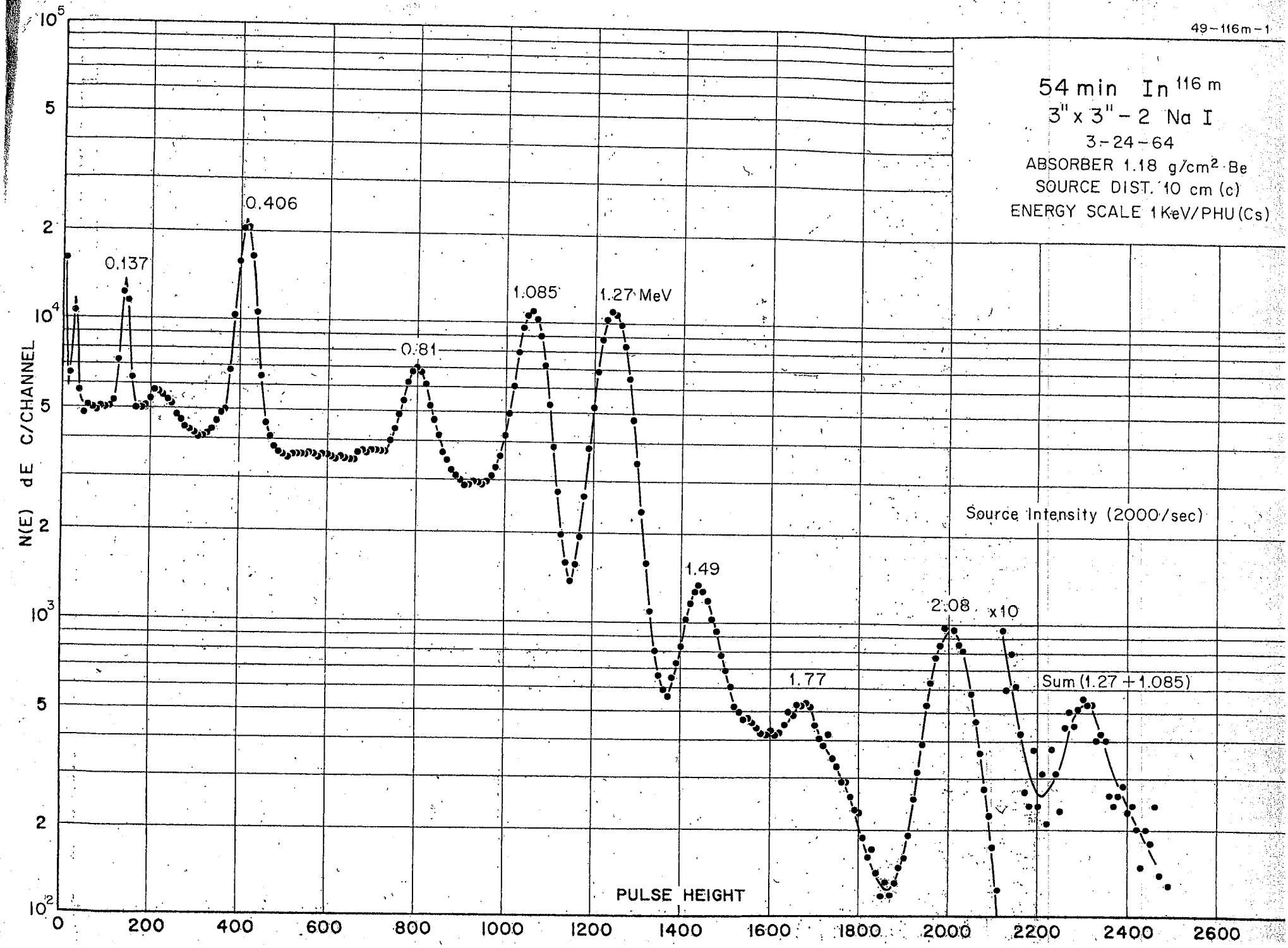

ORIGINAL

NUCLEAR ENGINEERING LABORATORY
NE E4710-4711

SAFE HANDLING OF RADIOACTIVE MATERIAL

1. Safety Rules: Handling of any radioactive material requires obeying certain safety rules and regulations. For the purpose of the experiments carried out in this laboratory, the following elementary safety rules are a must for the students involved in radioactivity work: A film badge and/or dosimeters have to be worn by each person involved. Regardless of dose, rubber gloves are always to be worn when directly handling radioactive materials in order to avoid contamination. Any radiochemical processing must be done in a well vented hood. Before performing any experiment, the students should always check the shielding thickness and/or the lengths of the tongs required so that the total dose received be less than the permissible dose. The survey meters should be calibrated and checked for proper operation before being used.

2. Radiation Quantities and Units: The roentgen is one of the earliest units of measuring radiation. Its most up-to-date definition is the definition is the exposure of X- or gamma-radiation so that the associated corpuscular emission (electrons produced by the X- or gamma-rays) per 0.001293 gram of air produces, in air, ions carrying one esu of electricity of either sign. Often, there arises confusion on what actually is the quantity whose unit is the roentgen. It should become clear that the roentgen measures the ability of radiation to ionize air and not the intensity of radiation or the energy absorbed directly. The quantity related to the local biological and chemical effects of radiation is the absorbed dose (the quantity of radiation absorbed per unit mass by the body or by any portion of the body. The unit of this quantity

For heavy particles, B is given by:

$$B = Z\left[\ln \frac{2mv^2}{I} - \ln(1-\beta^2) - \beta^2\right]$$

where $Z$ = atomic number of the absorber

$\beta$ = v/c (c = velocity of light in vacuum)

$I$ = geometric-mean excitation and ionization potential of absorbing atoms.

For electrons, B is almost constant for E up to nearly 0.5 Mev. Therefore,

$$\left(\frac{dE}{dx}\right)_c \sim \frac{1}{v^2}$$

The rate of energy loss passes through a minimum at about 1 Mev, and rises as the logarithm of E above 3 MW. If $I_m$ denotes the specific ionization and $\omega$ the energy loss per ion pair formed, or approximately 34ev for electrons in air, then one can write:

$$\left(\frac{dE}{dx}\right)_c = \omega I_m$$

a. Heavy particles. The heavy particles lose energy by excitation, mostly by ionization, and very little by other processes. An important property of the heavy particles is that they are initially monoenergetic. Of the heavy particles, the alphas were extensively studied and there exist fairly accurate empirical range formulae for them. Such a formula which is better than 1% accurate for the energy range 4-11 Mev and better than 4% accurate for the range 11-15 Mev is the following one:

$$R(cm) = [0.005E\ (Mev) + 0.285]\ E^{3/2}$$

This formula is for air at normal conditions (15 ° C and 760 mm Hg).

At lower energies:

$$R \propto E^{3/2}$$

At higher energies: $R \propto E^2$

It was noticed that for various absorbing materials, the quantity $\frac{R\rho}{\sqrt{A}}$ is approximately constant. Therefore, one can find the range in various substances by comparison with the range in air. For this purpose, the Bragg-Kleeman formula is good to approximately 15%:

$$R_1(cm) \cong 3.2 \times 10^{-4} \frac{\sqrt{A_1}}{\rho_1 (g/cm^3)} R_{air}(cm)$$

Range formulas for other (than alpha) heavy particles can be derived from the general range formula.

For an energy decrement from $E_1$ to $E_2$:

$$R_{ZM}(E_1 - E_2) = -\int_{E_2}^{E_1} \frac{dE}{(dE/dx)} = \frac{Mm}{4\pi e^4 z^2 ZN} \int_{v_2}^{v_1} \frac{v^3 dv}{B(v)}$$

If $v_2 = 0$:

$$R_{ZM}(v) = \frac{M}{z^2} F(v)$$

Where F(v) is essentially the above integral evaluated between 0 and v.

Finally, we can write for protons for example:

$$R_p(v) = \frac{R_p z_\alpha^2}{M_\alpha z_p^2} R_\alpha(v) - C$$

Where, in air, at normal conditions, c = 0.20 cm for E $\gtrsim$ 500 Kev and
c = 0.02 cm for E = 6.7 Kev

Hence, in air, at normal conditions and E > 500 Kev:

$$R_p(v) = 1.007\, R_\alpha(v) - 0.20 \text{ cm}$$

Since for the non-relativistic case: $E_p = \frac{E_\alpha M_p}{M_\alpha}$, we can also write:

$$R_p(E_p) = 1.007\ R_\alpha(3.972\ E_p) - 0.2\ \text{cm}$$

where $R_\alpha(3.972\ E_p)$ means that the alpha particle range is evaluated at $3.972\ E_p$.

For the same Z but different M, we can write

$$R_{ZM}(E) = \frac{M}{M_0} R_{ZM_0}(E') \qquad \text{where}: E' = \frac{EM_0}{M}$$

b. <u>Fission fragments</u>: They are nucleides of mass number between 72 and 160. They differ from the alpha particles in that their net charge decreases continuously during slowing down and that due to their increased nuclear charge, the nuclear collisions are important. An empirical formula giving the range of a fission fragment and which is accurate to 10% is the following one:

$$R\ (\text{mg/cm}^2) = KE^{2/3}\ (\text{Mev})$$

where the value of K varies for various materials:

| Material | K |
|---|---|
| Air | 0.14 |
| Al | 0.19 |
| Au | 0.50 |

c. <u>Electrons</u>: In this paragraph, the beta particles (electronn emitted from radioactive decay of nuclei) are also included.

Due to their small weight, the electrons have very complicated (non-linear) paths and for this reason, their ranges differ very much from their pathlengths. Electrons lose energy to the absorbers by excitation and ionization like the heavy charged particles but also by

another process called Bremsstrahlung (electromagnetic radiation). The rate of energy loss due to radiation is given by the approximate relation

$$\left(\frac{dE}{dx}\right)_r \cong Z^2 N (E + mc^2)$$

Where:

E = atomic number of the absorber
N = density of the absorber
E = electron energy
$mc^2$ = equivalent rest mass of the electron (0.51 Mev)

For the sake of comparison, the ratio of the radiative to collision energy loss is given by:

$$\frac{\left(\frac{dE}{dx}\right)_r}{\left(\frac{dE}{dx}\right)_c} \simeq \frac{Z\,E\,(Mev)}{700}$$

Bremsstrahlung becomes important only in the Bev energy range. In order to calculate the electron ranges, two empirical formulas can be used:

1. $R\,(mg/cm^2) = 412\,E^{1.265 - 0.0954 \ln E\,(Mev)}$ for $0.01\ Mev < E < 3\ Mev$ and

2. $R = 530\,E - 106$ for $1\ Mev < E < 20\ Mev$

For $E_m$ (maximum beta energy) between 0.1 and 4 Mev, the relative intensity in the absorption curve for a specific beta-particle can be fairly well represented by the formula :

$$\text{Relative intensity} = e^{-\frac{17\,d_m}{E_m^{1.14}}}$$

The special unit of absorbed dose is the "rad."

$$1 \text{ rad} = 100 \text{ erg/g} = 1/100 \text{ Joule/kg}$$

Absorbed Dose Rate is the quotient of $\Delta D$ by $\Delta t$, where $\Delta D$ is the increment in absorbed dose in time $\Delta t$

$$\text{Absorbed dose rate} = \frac{\Delta D}{\Delta t}$$

Special units: rad/d, rad/min, rad/h, etc.

Particle Fluence or Fluence ($\Phi$) of particles is the quotient of $\Delta N$ by $\Delta a$, where $\Delta N$ is the number of particles that enter a sphere of cross-sectional area $\Delta a$

$$\Phi = \frac{\Delta N}{\Delta a}$$

Particle Flux Density or Flux Density ($\varphi$) of particles is the quotient of $\Delta \Phi$ by $\Delta t$, where $\Delta \Phi$ is the particle fluence in time $\Delta t$:

$$\varphi = \frac{\Delta \Phi}{\Delta t}$$

It can also be referred to as "particle fluence rate."

Energy Fluence (F) of particles is the quotient of $\Delta E_F$ by $\Delta a$, where $\Delta E_F$ is the sum of the energies, exclusive of rest energies, of all the particles which enter a sphere of cross-sectional area $\Delta a$:

$$F = \frac{\Delta E_F}{\Delta a}$$

Energy Flux Density or Intensity (I) is the quotient of $\Delta F$ by $\Delta t$, where $\Delta F$ is the energy fluence in time $\Delta t$:

$$I = \frac{\Delta F}{\Delta t}$$

It can also be referred to as "energy fluence rate."

Kerma (K) is the quotient of $\Delta E_k$ by $\Delta m$, where $\Delta E_k$ is the sum of the initial kinetic energies of all the charged particles liberated by indirectly ionizing particles in a volume element of a specified material, $\Delta m$ is the mass of the matter in that volume element;

$$K = \frac{\Delta E_k}{\Delta m}$$

Note: $\Delta E_k$, the sum of the initial kinetic energies of the charged particles liberated by indirectly ionizing particles, includes not only the kinetic energy that these particles expend in collisions but also the energy they radiate in bremsstrahlung. Also, the energy of any charged particles is included where these are produced in secondary processes occurring within the volume element. Thus, the energy of the Auger electrons is part of $\Delta E_k$.

The kerma rate for a specified material is convenient to describe the field of indirectly ionizing particles for the purpose of dosimetry.

When charged particle equilibrium exists at the position and in the material of interest and bremsstrahlung losses are negligible, the kerma is also useful in dosimetry and is then equal to the absorbed dose at that point.

At high energies of X, gamma rays or neutrons, the kerma is less than the absorbed dose. In general, if the range of directly ionizing particles becomes comparable with the mean free path of the indirectly ionizing particles, no equilibrium will exist.

Kerma rate is the quotient of $\Delta k$ by $\Delta t$, where $\Delta k$ is the increment in kerma in time $\Delta t$.

Exposure (X) is the quotient of $\Delta Q$ by $\Delta m$, where $\Delta Q$ is the sum of the electrical charges on all the ions of one sign produced in air when all the electrons (negations and positions), liberated by photons in a volume element of air whose mass is $\Delta m$ are completely stopped in air:

$$X = \frac{\Delta Q}{\Delta m}$$

The special unit of exposure is the roentgen (R)

$$1R = 2.58 \times 10^{-4} \text{ Coulomb/kg} = 1 \text{ esu/0.001293 g air}$$

Note: $\Delta Q$ does not include ionization arising from the absorption of bremsstrahlung emitted by the secondary electrons.

Exposure Rate is the quotient of $\Delta X$ by $\Delta t$, where $\Delta X$ is the increment in exposure in time $\Delta t$.

$$\text{Exposure Rate} \quad \frac{\Delta X}{\Delta t}$$

Special units: R/s, R/min, R/h, etc.

Mass Attenuation Coefficient $(\mu/\rho)$ of a material for indirectly ionizing particles is the quotient of dN by the product of $\rho$, N and dl, where N is the number of particles incident normally upon a layer of thickness dl and density $\rho$ and dN is the number of particles that experience interactions in this layer

$$\frac{\mu}{\rho} = \frac{1}{\rho N} \frac{dN}{dl}$$

The term "interactions" means processes whereby the energy or direction of the indirectly ionizing particles is altered.

For X or gamma radiations:

$$\frac{\mu}{\rho} = \frac{\tau}{\rho} + \frac{\sigma}{\rho} + \frac{\sigma_{coh}}{\rho} + \frac{\kappa}{\rho}$$

where: $\frac{\tau}{\rho}$ = mass photoelectric attenuation coefficient.

$\frac{\sigma}{\rho}$ = total Compton mass attenuation coefficient.

$\frac{\sigma_{coh}}{\rho}$ = mass attenuation coefficient for coherent scattering

$\frac{\kappa}{\rho}$ = pair-production mass attenuation coefficient

Note: In the above equation, it is assumed that the nuclear interactions are not important which is true for X- or gamma-rays of energy of a few Mev's.

<u>Mass energy transfer coefficient</u> $\left(\frac{\mu_k}{\rho}\right)$ of a material for indirectly ionizing particles is the quotient of $dE_k$ by the product of $E$, $\rho$ and $dl$, where E is the sum of the energies (excluding rest energies) of the indirectly ionizing particles incident normally upon a layer of thickness dl and density $\rho$ and $dE_k$ is the sum of the kinetic energies of all the charged particles liberated in this layer

$$\frac{\mu_k}{\rho} = \frac{1}{E\rho}\frac{dE_k}{dl}$$

The relation between energy fluence and kerma may be written as:

$$K = F\frac{\mu_k}{\rho}$$

For X-or gamma-rays of energy $h\nu$

$$\frac{\mu_k}{\rho} = \frac{\tau_a}{\rho} + \frac{\sigma_a}{\rho} + \frac{\kappa_a}{\rho}$$

[Nuclear interactions are here neglected]

where:

$$\frac{\tau_a}{\rho} = \frac{\tau}{\rho}\left(1 + \frac{\delta}{h\nu}\right)$$

($\frac{\tau}{\rho}$ = the photoelectric mass attenuation coefficient, $\delta$ = average energy emitted as fluorescent radiation per photon absorbed.) and

$$\frac{\sigma_a}{\rho} = \frac{\sigma}{\rho} \frac{E_e}{h\nu}$$

($\frac{\sigma}{\rho}$ = total Compton mass attenuation coefficient,
$E_e$ = average energy of the Compton electrons per scattered photon.) and

$$\frac{K_a}{\rho} = \frac{k}{\rho}\left(1 - \frac{2mc^2}{h\nu}\right)$$

($\frac{k}{\rho}$ = mass attenuation coefficient for pair production, $mc^2$ electron rest energy.)

<u>Mass energy - absorption coefficient</u> $\left(\frac{\mu_{en}}{\rho}\right)$ of a material for indirectly ionizing particles is $\frac{\mu_k}{\rho}(1-G)$ where G is the proportion of the energy of secondary charged particles that is lost to Bremsstrahlung in the material.

Notes: For air, $\frac{\mu_{en}}{\rho}$ is proportional to the quotient of exposure by fluence.

$\frac{\mu_k}{\rho}$ and $\frac{\mu_{en}}{\rho}$ do not differ appreciably unless the kinetic energies of the secondary particles are comparable with or larger than their rest energy.

<u>Mass stopping power</u> $\left(\frac{S}{\rho}\right)$ of a material for charged particles is the quotient of $dE_s$ by the product of dl and $\rho$, where $dE_s$ is the average energy lost by the charged particle of specified energy in traversing a path length dl, and $\rho$ is the density of the medium:

$$\frac{S}{\rho} = \frac{1}{\rho} \frac{dE_s}{dl}$$

Note: $dE_s$ denotes energy lost due to ionization, electronic excitation and radiation. When bremsstrahlung losses are to be excluded, must be multiplied by an appropriate factor less than unity.

Linear Energy Transfer (L) of charged particles in a medium is the quotient of $dE_L$ by dl where $dE_L$ is the average energy locally imparted to the medium by a charged particle of specified energy in traversing a distance dl.

$$L = \frac{dE_L}{dl}$$

Note: The stopping power refers to energy imparted within a limited volume while the linear energy transfer refers to the loss of energy regardless of where this energy is absorbed.

Average energy (W) expended in a gas per ion pair formed is the quotient of E by $N_W$ where $N_W$ is the average number of ion pairs formed when a charged particle of initial energy E is completely stopped by the gas.

$$W = \frac{E}{N_W}.$$

Note: Ions arising from the absorption of Bremsstrahlung emitted by the charged particles are not included in $N_W$.

Activity (A) of a quantity of a radioactive nucleide is the quotient of $\Delta N$ by $\Delta t$, where $\Delta N$ is the number of nuclear transformations which occur in this quantity in time $\Delta t$.

$$A = \frac{\Delta N}{\Delta t}$$

Special unit of activity: Curie (Ci)

$$1 \text{ Ci} = 3.7 \times 10^{10} \quad s^{-1} \quad \text{(exactly)}$$

| Name | Symbol | Dimensions | UNITS MKSA | UNITS cgs | Special |
|---|---|---|---|---|---|
| Kerma rate | .... | $EM^{-1}T^{-1}$ | $JKg^{-1}s^{-1}$ | $erg\ g^{-1}\ s^{-1}$ | |
| Exposure | X | $QM^{-1}$ | $CKg^{-1}$ | $esu\ g^{-1}$ | R (Roentgen) |
| Exposure rate | .... | $QM^{-1}T^{-1}$ | $CKg^{-1}s^{-1}$ | $esu\ g^{-1}s^{-1}$ | $Rs^{-1}$, etc. |
| Mass attenuation coeff. | $\frac{\mu}{\rho}$ | $L^2\ M^{-1}$ | $m^2\ Kg^{-1}$ | $cm^2\ g^{-1}$ | |
| Mass energy Transfer coeff. | $\frac{\mu_k}{\rho}$ | $L^2\ M^{-1}$ | $m^2\ Kg^{-1}$ | $cm^2 g^{-1}$ | |
| Mass energy absorption coeff. | $\frac{\mu_{en}}{\rho}$ | $L^2\ M^{-1}$ | $m^2\ Kg^{-1}$ | $cm^2\ g^{-1}$ | |
| Mass stopping power | $\frac{S}{\rho}$ | $EL^2\ M^{-1}$ | $Jm^2\ Kg^{-1}$ | $erg\ cm^2\ g^{-1}$ | |
| Linear energy transfer | L | $EL^2$ | $JM^{2l}$ | $erg\ cm^{-1}$ | KeV $(\mu m)^{-1}$ |
| Average energy per ion pair | W<br>W | E<br>E | J | erg | ev |
| Activity | A | $T^{-1}$ | $s^{-1}$ | $s^{-1}$ | Ci (Curie) |
| Specific Gamma-ray constant | $\Gamma$ | $QL^2\ M^{-1}$ | $Cm^2Kg^{-1}$ | $esu\ cm^2g^{-1}$ | $Rm^2h^{-1}Ci^{-1}$ |
| Dose equivalent | DE | | | | rem |

## APPENDIX 2

Formulas for Geometry Calculations

The "geometry" of the aperture for a point source, $G_p$, is defined as the fraction of the total solid angle subtended by the aperture, i.e.

$$G_p = \frac{\Omega_p}{4\pi}$$

For a point source and a detector with a circular aperture of radius R (the point source being on the axis of the aperture):

$$G_p' = \frac{1}{2}\left(1 - \frac{D}{\sqrt{D^2+R^2}}\right) \equiv \frac{1}{2}\left(1 - \frac{D}{L}\right),$$

Where D is the distance from the point source to the plane of the aperture,

For a point source off the axis of a circular aperture by a perpendicular distance equal to $\rho$ and $\rho/L < 1$,

$$G_p = G_p' - \frac{3}{8}\rho^2\frac{R^2 D}{L^5} + \frac{15}{32}\rho^4\frac{R^2 D}{L^9}\left(D^2 - \frac{3}{4}R^2\right) + \dots$$

$$= G_p' + \frac{1}{2}\frac{D}{L}\sum_{n=1}^{\infty}\frac{(-1)^n(2n+1)!}{2^{4n}(n!)^2}\left(\frac{\rho^2}{L^2}\right)^n\sum_{k=0}^{n} m_k$$

Where

$$m_k = \frac{(-1)^{k+1}(4n-2k)!}{(2n-k)!\,(2n-2k+1)!}\left(\frac{D^2}{L^2}\right)^{n-k}$$

and $G_p'$ is given by the above formula.